PAPERS IN PHYSICAL OCEANOGRAPHY AND METEOROLOGY

PUBLISHED BY

MASSACHUSETTS INSTITUTE OF TECHNOLOGY

AND

WOODS HOLE OCEANOGRAPHIC INSTITUTION

VOL. VI, NO. 2

CIRCULATION IN UPPER LAYERS OF SOUTHERN NORTH ATLANTIC DEDUCED WITH USE OF ISENTROPIC ANALYSIS

BY

R. B. MONTGOMERY

Contribution No. 190 from the Woods Hole Oceanographic Institution

CAMBRIDGE AND WOODS HOLE, MASSACHUSETTS

August, 1938

CONTENTS

PREFACE

The following paper is a revised form of a thesis prepared under the supervision of Professor C.-G. Rossby and submitted at Massachusetts Institute of Technology; it is published under the Faculty's authorization.

During the prosecution of the research the author enjoyed the facilities of the Massachusetts Institute of Technology and the Woods Hole Oceanographic Institution. Besides unpublished observations made by the latter institution, the author wishes to acknowledge, to the Department of Terrestrial Magnetism of the Carnegie Institution of Washington, the opportunity of incorporating in this study the serial observations at stations 18–30 made with *Carnegie* in 1928.

The author has benefited by valuable consultations with Professor C. O'D. Iselin of Harvard University and with Professor A. E. Parr of Yale University. He wishes to acknowledge especially the stimulating guidance of Professor Rossby.

I. INTRODUCTORY STATEMENT

Except for the presence in most localities of a shallow homogeneous surface layer and of a relatively homogeneous and deeper bottom layer, the oceans of the temperate and tropical regions are stratified and vertically stable at all depths. Due to the opacity of water for long-wave radiation and to the damping of vertical turbulence by the stability, there is no potent mechanism for altering the potential density of any water element below the layer of direct surface influences. Hence there can be no flow of major proportions across surfaces of constant potential density. For these reasons it is now generally accepted that flow takes place essentially parallel to these surfaces. It follows that the major sources for the water on each surface of constant potential density are to be found along its intersection with the sea surface in higher latitudes.

II. SCOPE OF THE STUDY AND RÉSUMÉ OF PREVIOUS INVESTIGATIONS RELATING TO ATLANTIC EQUATORIAL CURRENTS

The Equatorial Current appears to be of prime importance in the general circulation of the North Atlantic Ocean. This is deduced from the following elementary considerations. The similarity between the anticyclonic atmospheric circulation over the Atlantic and the anticyclonic oceanic circulation, and the inadequacy of direct thermal circulation within the ocean, strongly suggest that the ultimate major cause of the circulation of the upper layers of the ocean (upper 1000 meters or so) is the force exerted by the wind on the surface. Furthermore, there is reason to expect that most of the momentum of the oceanic circulation is received in the trade wind region. In that event the North Equatorial Current would be the connecting link between the trades and the general circulation of the North Atlantic, and becomes, perhaps, the current system of most importance in the understanding of this general circulation.

The aims of the present study are two, the first being to contribute to the descriptive knowledge of the North Equatorial Current and its environs by use of the principles mentioned in the Introductory Statement. These principles, in spite of their validity being almost self-evident, have often been disregarded in oceanography, and their full significance has not been previously stated. Accordingly the second aim is to test further the general validity and usefulness of these principles, for which purpose the specific region under investigation serves as a good example.

The recent reports of most importance dealing in part with the circulation of the upper layers of the southern North Atlantic are by Jacobsen (1929), Iselin (1936) and Defant (1936). The last is not only of particular interest in connection with the principles put forward in the present paper, but it is also by far the most comprehensive and detailed treatment of this region. Use was made of all the sub-surface observations now available with the principal exception of the 1937 *Atlantis* material. The following review of Defant's report appears suitable as a groundwork for the subsequent discussion.

The division of the ocean into an upper troposphere and a lower stratosphere is considered by some merely an arbitrary convenience which separates the warm, relatively saline troposphere, which contains the strong oceanic circulation, from the cold and less saline and slowly moving stratosphere, which contains most of the ocean water. Such a boundary could be arbitrarily defined, for instance, by the isothermal surface of 8°.

Defant, however, identifies the boundary with a slightly developed discontinuity in temperature and salinity which rises to the sea surface at the polar fronts. In low latitudes the discontinuity is hardly perceptible, but here the boundary is identified with the principal oxygen minimum. The low oxygen values in the O_2-minimum are attributed to very slow renewal of water, so that, according to Defant, the boundary between troposphere and stratosphere is a surface of practically no motion, in fact of less motion than the stratosphere. The boundary so deduced coincides roughly with the 8°-isotherm, and nowhere exceeds the depth of 1000 meters. According to Seiwell (1937b, p. 14) the O_2-minimum coincides closely with the $\sigma_t = 27.23$-surface everywhere in the western North Atlantic. In the same paper Seiwell demonstrates the lack of strong evidence that the O_2-minimum layer is relatively motionless.

The troposphere, as defined above, is divided by Defant into three layers: a surface homogeneous layer which is not everywhere present, a middle layer of strong stability ("Troposphärische Sprungschicht," its top and bottom defined by a vertical temperature gradient of 0.02° per meter), and a lower layer called the subtroposphere.

The first descriptive method used by Defant in deducing the circulation of the troposphere is based on an analysis of the maximum vertical density gradient within the middle layer of strong stability. It is assumed that to a first approximation this surface is a discontinuity separating motionless homogeneous water below from homogeneous water above. (It would have been sufficient to assume each layer horizontally homogeneous.) The magnitude of the discontinuity is taken to be the difference between the density at the bottom of the middle layer of strong stability and the mean density of the surface layer. From the slope of the discontinuity, taken off a chart giving its depth, and from its magnitude the gradient current in the surface layer was computed and the results represented on a chart (Defant's Beilage XXXVIII). A dome in the discontinuity corresponds to cyclonic motion, a depression to anticyclonic motion.

While there is no reason to doubt the broad features of the current pattern deduced by this method, it appears that some of the details are insignificant. Observations from expeditions widely spaced in time have been used, which is especially untrustworthy for any application of dynamic calculations (note for instance the weight given in his charts to the value for *Carnegie* station 24 at 8°N. 36°W. made in August 1928 and the resulting contrast with *Meteor* stations made in February and April 1927). Internal waves exert a disturbing effect, which however is partially eliminated for *Meteor* stations due to the repetition of serial observations. Furthermore, the simplifying assumption of a discontinuity is not very close to fact, hence especially it would appear that the determination of the depth of the hypothetical discontinuity in terms of the maximum gradient is uncertain and at nearby stations might occur at very different σ_t-values.

The surface of maximum density gradient does not correspond closely to a σ_t-surface but occurs at considerably higher σ_t-values in the subtropics than in equatorial regions. From a comparison with Chart 8 below it appears to coincide very roughly, in the region between the equator and 30°N., with the $\sigma_t = 26$-surface.

Defant's report is the first to attempt a complete description and explanation of the general features of the equatorial currents of the Atlantic Ocean. In view of the almost complete lack of definite knowledge concerning the dynamic system maintaining the general circulation of the ocean, it is not surprising to find that some of his key statements appear untenable. In the present study, it must be admitted, no such comprehensive goal is attempted.

The North and South Equatorial Currents are attributed, as is now generally accepted, to the action of the northeast and southeast trades. The presence of the Equatorial Counter Current (and its eastward extension as the Guinea Current) between the two equatorial currents is considered, following Sverdrup (1934), a phenomenon which is necessary in order that, under the external conditions of trade winds asymmetric about the equator, gradient currents of infinite velocity should not occur at the equator. Along the equator, according to Sverdrup, there must be a trough (or a ridge) in the sea surface so that velocity may be continuous across the equator. Further: "If these currents [North and South Equatorial Currents] are asymmetric in respect to the equator . . . the centre line of the trough will be found at some distance from the equator, and the surface would show a definite inclination across the equator if no compensation took place. If the system is to be dynamically stable, such a compensation must be found and it can be shown that the simplest form of compensation leads to the development of a countercurrent of the observed character," i.e. with two troughs in the sea surface as in Figure 2 below. There is no obvious justification for the statement that "the centre line of the trough will be found at some distance from the equator;" rather, if the mass distribution is free to adjust itself to the current distribution, any system of pure west equatorial currents would result in a topography of the sea surface with a single trough, not necessarily symmetrical, at the equator. If the mass distribution is not free to adjust itself to the current system, Sverdrup's theory is not complete without explaining in more detail why this lack of adjustment should result in a counter current of the observed character. From another point of view, since it now appears that counter currents are of general occurrence in all latitudes, it seems unlikely that the Equatorial Counter Current can be ascribed to the vanishing of the Coriolis force at the equator.

The pure drift current resulting from the northeast trades has a net transport whose major component is directed poleward. In order to account for the necessary compensation in the form of an equatorward component at some lower level, Defant considers the simplified case of a canal running east-west. Axes x, eastward, and y, northward, are chosen. Since v (northward component of velocity) must vanish at both walls of the canal, it is assumed that both u and v are proportional to sin $(\pi y/b)$, where b is the width of the canal, so that the horizontal motion along all verticals is identical except for this factor depending on y. For all particles below the sea surface balance is assumed to exist between the equatorward pressure gradient, the deflecting force and the shearing stress across horizontal surfaces. It is assumed that the eddy viscosity coefficient is constant at 100 cm.$^{-1}$g.sec.$^{-1}$, that shearing vanishes at the depth of frictional influence, and that continuity for motion in the y-direction is maintained above this depth. As the final boundary condition for the North Equatorial Current, for the center of the canal at 15°N. a surface velocity of $u=-15$ and $v=3$ cm.sec.$^{-1}$ is used. Defant presents the velocities computed from his solution for four depths and I have drawn these in Figure 1. The inappropriateness of this result is at once apparent, for it represents the superposition of a uniform west gradient current of 18 cm.sec.$^{-1}$ on the drift current produced by a *south* wind. It is furthermore obvious that for the assumed conditions a steady state of motion cannot exist under an east wind, for no force is taken into account which can balance its stress on the sea surface. It was exactly this type of situation which led Rossby to the conclusion that lateral shearing stresses are of prime importance in oceanic dynamics (1936, pp. 5–6).

The same analysis is assumed to apply also to canals corresponding to the northern

and southern branches of the South Equatorial Current. The circulation Defant proposes for the canal of the Counter Current, however, would have to be associated with a *north* wind. His schematic representation of the meridional and vertical components of flow is reproduced in Figure 2. Ascending motion is indicated at the equator and at the boundary

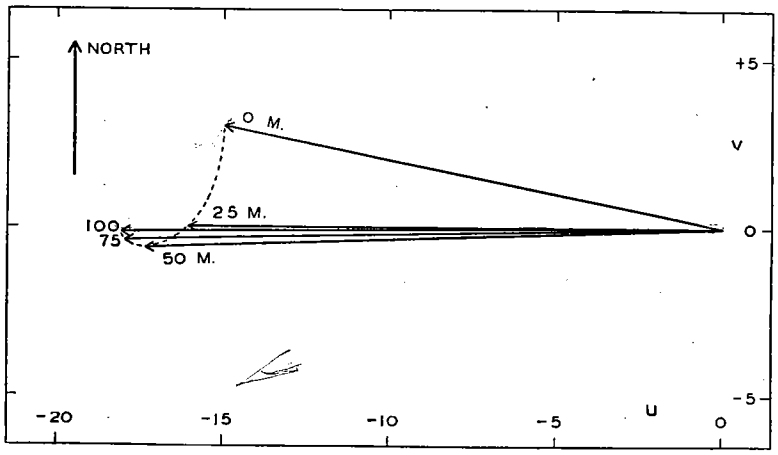

FIG. 1.—Vertical distribution of velocity in the North Equatorial Current as computed by Defant.

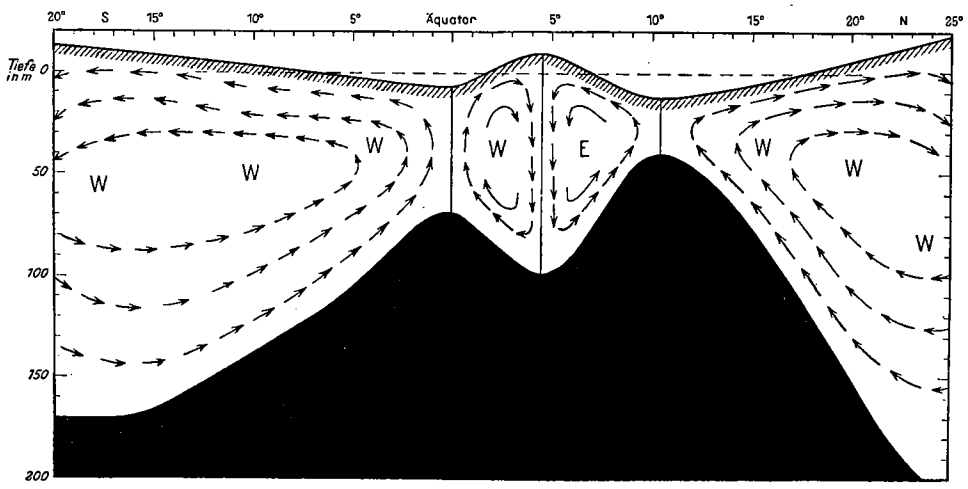

FIG. 2.—Schematic representation of the zonal and meridional components of motion in the troposphere of the Atlantic Ocean, according to Defant (1936, Abb. 62). Position of the density discontinuity drawn to scale, position of the sea surface exaggerated 100 times.

between the North Equatorial Current and the Counter Current (10°N.), and descending motion at the boundary between the South Equatorial Current and the Counter Current (5°N.). Aside from the false theoretical basis, two other objections may be raised against this schematic representation. The first refers to the positions of the subtropical convergences, which are indicated as lying outside the range of the diagram. According to other diagrams in Defant's paper, the convergences are represented as *lines* of convergence (following earlier writers) roughly coinciding with the 30th parallels. Actually,

as shown elsewhere (Montgomery, 1936, Fig. 1), there is a continuous zone of convergence of the drift current from about 12°N. to about 35°N., and the greatest convergence occurs at about 17°N.

The other objection refers to the simplification of the problem in assuming that the whole upper layer above the maximum density gradient is homogeneous. Since this is actually not the case, it has yet to be shown how vertical motion can take place through potential density surfaces. It seems possible to explain a certain amount of ascending motion at the equator and at 10°N., where the upper layer is so shallow that water from even its deepest part might be "mixed upward" by vertical turbulence induced at the sea surface (See Chapter XIII). But it does not seem possible to explain the increase of density along the streamlines involved in the descending motion at the subtropical convergences and at 5°N. At the northern subtropical convergence, according to one of Defant's diagrams, no horizontal motion is indicated, while the descending motion extends to a depth of 600 meters; below about 200 meters this descending water spreads both southward and northward. The accompanying values are from Defant's composite

Depth in meters	0	100	200	300	400	500	600
σ_t	26.1	26.1	26.3	26.5	26.7	26.8	27.0

meridional section of observed conditions at this convergence; that continuous sinking should take place through this water column is entirely contrary to the principles outlined in the Introductory Statement.

To go back to the summary of Defant's descriptive methods of studying horizontal circulation, mention should be made of his chart showing the depth of the secondary maximum in the vertical temperature gradient (his Abb. 67). This surface occurs below the principal maximum of the density gradient discussed above, and he identifies it with the boundary between the troposphere and stratosphere and hence with the O_2-minimum layer. It supposedly occurs, then, at about $\sigma_t = 27.23$. However, as may be seen from a comparison with the topography of the $\sigma_t = 27$-surface shown below on Chart 2, in some regions the secondary maximum in vertical temperature gradient occurs above $\sigma_t = 27$. The circulation above this temperature gradient was deduced in the same manner as for the principal maximum of the density gradient. (This chart will be mentioned further in Chapter VII.)

The second descriptive method is based on the geographical distribution of salinity at the depth of maximum salinity. This is a case of the general "Kernschicht" method which served as the chief tool in Wüst's (1935) study of the stratosphere of the Atlantic Ocean. Defant concludes that the water constituting the S-maximum has its origin in the deepest part of the subtropical reservoirs of water of high salinity, because at the equatorward boundaries of the reservoirs the depth of the salinity maximum coincides with the depth of the salt surface layer of the reservoir. On his chart showing salinity distribution at the S-maximum, two predominantly zonal areas a few degrees in width occur at about 2°S. and 11°N. where the S-maximum is absent. These are due, according to Defant, to the ascending motion at the equator and at the boundary between the North Equatorial Current and the Counter Current. The flow pattern deduced from the salinity distribution, interpreted according to the scheme of zonal, meridional and vertical circulation outlined above, is reproduced here in Figure 3. It will be discussed in detail in Chapter IX.

Defant emphasizes that the S-maximum occurs within the middle layer of strong stability, usually just above the surface of maximum stability, and that this explains why

the water of high salinity can travel so far without losing its identity by vertical mixing. He concludes, in fact, that in the regions of strongest development of vertical density gradient the stability is so great that the vertical eddy viscosity vanishes completely.

Defant's use of the S-maximum distribution involves the assumption, which he does not discuss, that the S-maxima occur on a continuous surface and that the surface is at a fairly constant density. In a general way this assumption is certainly justified, but in some cases it might lead to false conclusions. Of the 286 oceanographic stations which I utilize in the work to be described below, 194 show S-maxima, with the distribution

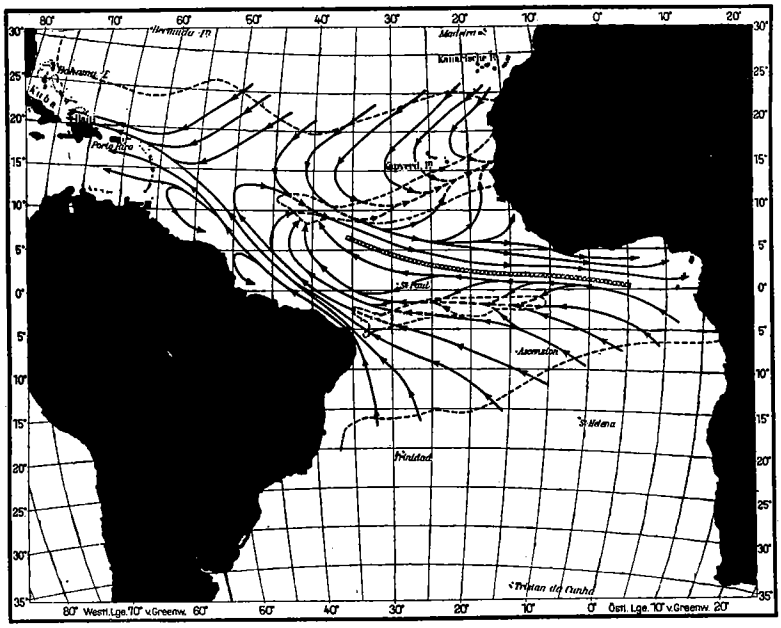

FIG. 3.—Current distribution in the S-maximum layer as deduced from the salinity distribution in this layer, according to Defant (1936, Beilage XLV). The broken line outlines the northern and southern limits of the sub-surface S-maximum layer, as well as two narrow zonal areas where it is absent. The crosshatched line represents the divergence line at the southern edge of the Equatorial Counter Current and Guinea Current.

given in Table 1 (determined from the smooth t-S-curve for each station). All the stations included lie between the equator and 30°N. Although maxima occur over a large range of σ_t, 130 of the cases occur between $\sigma_t = 25.0$ and $\sigma_t = 25.8$, a comparatively limited range. The mean value is $\sigma_t = 25.4$, which is the same as Parr (1938b) finds for the southwestern North Atlantic and the Caribbean.

TABLE 1

FREQUENCY DISTRIBUTION OF S-MAXIMUM WITH REGARD TO σ_t

σ_t	24.0	24.1	24.2	24.3	24.4	24.5	24.6	24.7	24.8	24.9	25.0	25.1	25.2	25.3	25.4	25.5	25.6	25.7	25.8	25.9	26.0	26.1	26.2	26.3	26.4
Cases	2	0	1	4	2	3	2	6	6	3	10	12	11	9	18	14	25	15	16	8	9	9	4	4	1

The contribution of Defant's report which is found to be of prime importance is thus his study of the geographical distribution of salinity at the S-maximum. From this he has deduced certain features of the flow pattern by use of the fact that axes of tongues of high salinity must coincide with lines of flow.

III. ISENTROPIC ANALYSIS

As indicated in the Introductory Statement, the logical method of deducing oceanic flow patterns from temperature, salinity and oxygen observations is to chart these properties for surfaces of constant potential density. The "Kernschicht" method, such as Defant's study of the distribution of maximum salinity, is equivalent to this method to the extent that the center of the "Kernschicht" lies on a surface of constant potential density. But, whereas there are only a limited number of "Kernschichts" in the ocean, there are an unlimited number of surfaces of constant potential density so that flow patterns may be studied at all depths. Another approximation to this method is the study of the salinity distribution on a surface of constant temperature, as used by Parr (1936, Fig. 2B; 1937, Fig. 44).

Some years ago Shaw (1930, pp. 259–264) suggested the use of isentropic charts, and actually constructed an isentropic weather map containing the topography of the isentropic surface and the isotherms on it, which he showed to be equivalent to isobars and isopycnals. He suggested the word "isentrope" to designate an isentropic surface. Shaw pointed out clearly the two primary properties of the isentrope, namely (1) that flow takes place along it in so far as conditions are adiabatic (and in so far as density is not altered by mixing), and (2) that it maintains its identity under adiabatic deformations with regard to pressure.

The first indication of the appropriateness of isentropic analysis for the study of geophysical *flow patterns*, which involves principally the distribution of dissolved substances (salt or oxygen in water, water vapor in air) on the surface of constant potential density, was however contained in Rossby's (1936) discussion of the dynamics of the Gulf Stream, which revealed the importance of lateral shearing stresses. From this Redfield (1936) has drawn a significant conclusion regarding the transfer of plant nutrients along such surfaces in the ocean. Isentropic analysis was applied by Rossby and collaborators (1937a, 1937b) and Namias (1938) to the deduction of flow patterns from aerological data. Subsequently Parr applied the method in two studies of oceanographic flow patterns, in one (1938a) using the salinity distribution, in the other (1938b) the temperature distribution, on surfaces of constant σ_t.

A third property of a surface of constant potential density, which follows as a corollary of property (1) above, may be stated as follows: Turbulent motion in a stratified medium tends to take place under hydrostatic equilibrium, hence the components of turbulence of greatest intensity are those lying in the surface of constant potential density. These components are referred to as lateral mixing in contradistinction to vertical mixing and also to mixing along strictly horizontal surfaces.

The results of the two papers by Rossby and collaborators which may be expected to be of especial import for the ocean are the following:

(1) The flow patterns obtained on isentropes are simpler and more stable than any representation of conditions on a horizontal surface.

(2) The charts studied furnish strong indications of intense isentropic mixing.

(3) The charts studied, which pertain to conditions on the south side of the main westerly current of the Northern Hemisphere, demonstrate a pronounced tendency for the currents to break up into large anticyclonic eddies.

(4) The currents tend to be parallel to the contour lines of the isentrope.

(5) It is emphasized that isentropic charts, in representing the geographical variation

of identifying properties (potential temperature and specific humidity), serve the same purpose as characteristic diagrams[1] (Rossby diagram) in representing their vertical distribution. The oceanic counterparts are the temperature-salinity and temperature-oxygen diagrams. (See also Parr, 1938a, p. 135.)

The properties and results mentioned above all refer to the use of isentropic analysis as a descriptive tool. While the descriptive use of isentropic analysis is of great importance in itself, one should not lose sight of its dynamic implications, and the fact that the origin of isentropic analysis in its present form sprang from theoretical studies.

Atmospheric isentropic analysis, as the word implies, is the study of conditions on a surface of constant entropy (computed from temperature and total pressure, hence neglecting the presence of water vapor). Air being, except for the presence of small quantities of water vapor, a uniform substance, this surface is equivalent to a surface of constant potential temperature and to one of constant potential density. Ocean water, on the other hand, is essentially a solution of two substances, water and salt, and the last two systems of surfaces not only intersect each other, but presumably both intersect surfaces of constant entropy. The one which has the advantageous properties of the atmospheric isentrope (except for the lack of uniqueness stated four paragraphs below) is the surface of constant potential density.

In regard to nomenclature, either of two precedents might be followed: the prior atmospheric use of "isentropic analysis" by Shaw and Rossby, which may be objected to on the ground that not all particles on an oceanic surface of constant potential density have the same entropy, or the subsequent oceanic use of "isopycnic analysis" by Parr, which may be objected to on the ground that a surface of constant *potential* density should not be called "isopycnic" and usually does not even approximately conform to a true isopycnic surface. The fundamental procedure in question, however, is to study the distribution of identifying properties with which a particle moving adiabatically without mixing, hence *isentropically*, under hydrostatic equilibrium may come in contact.[2] Hence it appears advantageous, especially for uniformity with the atmospheric use, to call the study of oceanic conditions on a surface of constant potential density "isentropic analysis," and the graphical representations of the surfaces "isentropic charts."

Actually, since potential density is so nearly equivalent to σ_t (except at pressures greater than 1000 decibars), it is sufficient to use the surface of constant σ_t. This is much more convenient, for in order to determine properties at a given potential density surface it would be necessary to convert all observed temperatures to potential temperatures. Unfortunately there is no single word to designate a surface of constant σ_t. It will be referred to hereinafter as a "σ_t-surface," which, though clumsy, is at least specific.[3]

In order to illustrate the error involved in using a σ_t-surface instead of a surface of constant potential density, the three stations in the following table may be examined.

---

[1] By characteristic diagram is meant one on which the two axes correspond to two identifying properties. Such atmospheric properties are potential temperature and specific humidity, oceanic ones are temperature (strictly potential temperature), salinity and specific oxygen content. On such a diagram the line joining all points corresponding to an atmospheric sounding or to an oceanographic station is the characteristic curve for the sounding or station.

[2] At first sight it may appear inconsistent to stipulate "without mixing," because the method is peculiarly adapted to the study of mixing, particularly lateral mixing. When lateral mixing takes place, however, the motion is no longer isentropic nor is it strictly parallel to surfaces of constant potential density, but is directed slightly toward surfaces of higher potential density, the effect known as cabbeling.

[3] For a water particle of salinity S and temperature t and at pressure p, the density may be written $\rho_{S,t,p}$. σ_t is defined as $1000(\rho_{S,t,0}-1)$, where $\rho_{S,t,0}$ is the density of water of salinity S and temperature t and at atmospheric pressure.

In the analysis which will follow the $\sigma_t = 27$-surface is the deepest utilized, and its extreme depths and extreme temperatures within the region studied occur at these three stations.

Station	P	t	S	θ	ρ_θ	t_{400}	ρ_{400}
Atlantis 1201	193	13.73	35.96	13.70	1.02701	13.76	1.02877
Bache 189	835	12.50	35.64	12.38	1.02703	12.43	1.02880
Meteor 297	400	8.25	34.67	8.21	1.02701	8.25	1.02883

The table gives, for $\sigma_t = 27$, the interpolated pressure in decibars (P), which is equivalent to depth in meters, temperature in °C. (t) and salinity in °/₀₀ (S). These are followed by potential temperature (θ) determined with the use of Ekman's (1905, Fig. 1) values for adiabatic cooling of sea water, and potential density (ρ_θ), or density corresponding to θ, S and $P = 0$, as determined with the use of Bjerknes' (1912) Hydrographic Tables. Since the range of potential density for the three samples is only 0.00002, the error is unimportant.

As mentioned elsewhere (Montgomery, 1937), one of the primary properties of the atmospheric isentrope, that it maintains its identity under adiabatic deformations, is not exactly fulfilled by an oceanic surface of constant potential density. This discrepancy may be evaluated for the three samples in the table above. If the first two were displaced adiabatically to 400 db., the pressure of the third sample, they would assume the temperatures (t_{400}) and densities (ρ_{400}) given in the last two columns of the table. The range of 0.00006 in ρ_{400} shows this effect to be larger than the one discussed in the last paragraph. The extent to which it might affect isentropic analysis may be illustrated by use of the vertical density gradient at 400 db. at *Meteor* 297, 0.00064 per 100 db., and of the adiabatic variation of density for the samples from *Atlantis* 1201 and *Bache* 189, 0.00043 per 100 db. If the sample from *Atlantis* 1201 were moved isentropically under hydrostatic equilibrium to *Meteor* 297, it would arrive at 371 db., surrounding salinity 34.71 °/₀₀, that from *Bache* 189 at 383 db., 34.69 °/₀₀. The differences between 34.71, 34.69, and 34.67 °/₀₀ are small compared with the differences between 35.96, 35.64 and 34.67 °/₀₀.

While it has been found that in the atmosphere flow takes place in general parallel to the contours of an isentrope, there is reason to expect that in the ocean the sense of the motion also will usually be prescribed by the contours of a σ_t-surface (Parr, 1938a, p. 148). If, as is often assumed, pressure gradients along a certain deep horizontal surface vanish, then on proceeding upward from this surface, as long as the isosteres slope in the same direction, the gradient current is parallel to the intersection of isosteric and equipotential surfaces with a prescribed sense. This is approximately true also for a σ_t-surface, that the gradient current is parallel to its contours, cyclonic about domes and anticyclonic about depressions. Since in most regions where there is a marked slope of the isosteres this slope has the same direction at all depths, this principle seems of quite general applicability except near the sea surface.

Defant's use of the topography of the surface of principal density gradient (cf. p. 6) was of course a specialization of the principle just stated. A quantitative method for determining and representing gradient currents on an σ_t-surface has been outlined (Montgomery, 1937). Although to date this has not been put into practice, the calculations have been carried out for a single line of stations and are presented below in Chapter V.

While it is useful, or even necessary, to have some knowledge of the gradient flow on a σ_t-surface, it should be emphasized that the basis of isentropic analysis is the deduction of flow patterns from the distribution of dissolved substances, which is entirely independent of any assumptions regarding gradient flow. While the descriptive result of

isentropic analysis is an end in itself, the method affords information necessary for dynamic studies, especially (1) the flow patterns and hence probably the deviations from gradient flow, and (2) the representation of dissolved substances proper for determining lateral mixing coefficients.

The published applications of isentropic analysis to the atmosphere have been for synoptic data only. Isentropic charts have also been prepared at the Massachusetts Institute of Technology and at the Weather Bureau in Washington using mean data for a month and for a natural period. On the other hand, the oceanographic data available for the North Atlantic is spread over a number of years, and the observations made within any short period of time are too few to study as an individual synoptic situation. Hence the procedure will be followed of assuming the oceanic circulation to be sufficiently constant so that the difference in time of observations is of secondary importance, a procedure used by Defant (1936, p. 291) also.

The Introductory Statement contained the qualitative result that radiation and vertical mixing appear ineffective below the layer of direct surface influence. In carrying out the isentropic analysis the hypothesis is followed that *the waters at every point of a given σ_t-surface are mixtures of the waters found at its intersection with the sea surface only*, in other words that radiation and vertical mixing are of secondary importance compared with lateral mixing. Although the degree of truth in this statement is as yet undetermined, the proper procedure nevertheless seems to be to first make the analysis on this basis and later try to determine whether the results are compatible with, especially, the amount of vertical mixing present.

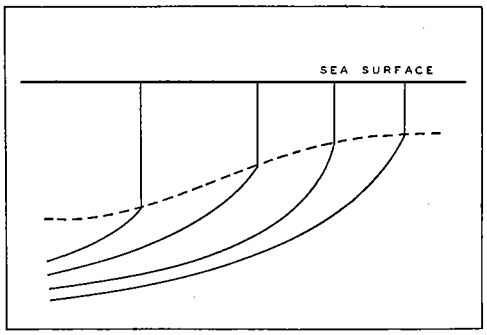

FIG. 4.—Schematic section representing lower boundary of surface influences and vertical mixing, shown by broken line. σ_t-surfaces are represented by full lines.

If this hypothesis is correct, it follows that where a σ_t-layer intersects the sea surface in a region of strong horizontal convergence of the surface layer there should be a strong source for the σ_t-layer. For quantitative equality to exist between convergence of surface water and the strength of the sources for σ_t-layers, it must be justifiable to assume that surface influences (radiation and precipitation, etc.) and vertical mixing are limited to a vertically homogeneous surface layer, so that conditions near the surface may be represented by a picture of the form shown in Figure 4. While this may obtain in regions of surface convergence, it probably does not in all regions of divergence. Surface divergence may bring the lower boundary of the homogeneous surface layer so near the sea surface that surface influences and vertical mixing are not confined to the surface layer (as mentioned on p. 9).

The principal part of the convergence of the surface layer is probably the convergence of the drift current. A computation of this has been made for the Atlantic between 15°N. and 55°N. for mean July conditions only (Montgomery, 1936), which may serve as a rough evaluation of the convergence of the surface layer.

IV. MATERIAL AND METHODS OF INTERPOLATION USED IN PLOTTING ISENTROPIC CHARTS

The study covers the Atlantic between the equator and 30°N., exclusive of the Central American seas and of the Gulf of Guinea. All hydrographic stations (for which the serial measurements included at least one of the σ_t-surfaces here studied) made within this region by the ships listed in Table 2 have been utilized. The position of each of the 286 stations is shown on Chart 1. Determinations of dissolved oxygen were not made on the *Carnegie*, *Bache*, *Discovery*, *Challenger*, *Michael Sars* and *Möwe* expeditions. For sources of the data, see page 48.

TABLE 2
DATES OF STATIONS

SHIP	YEAR	MONTH	STATIONS
Atlantis	1932	III–IV	1161–1182, 1194–1217
	1933	II	1468–1479
		III	1487–1491, 1516–1520
		V	1611–1617
	1937	I	2726–2750
Bache	1914	II	183, 185, 187, 189, 191, 193, 195
		III	205–212
Carnegie	1928	VIII–IX	18–30
Challenger	1933	IV	1324–1328
	1934	IV–V	1562–1566
		VII	1580–1581
	1935	IV	1668
		XI	1758, 1762–1763
Dana	1921	X	1156–1157, 1159
		XI	1160, 1162, 1164–1166, 1169, 1171–1174, 1176–1179, 1181–1182, 1185
	1922	I	1195
		II	1239, 1241–1242
		III	1261
		IV	1319, 1321–1322
		V	1333, 1335
		VI	1356, 1362
Deutschland	1911	VI–VII	12–26
Discovery	1927	VIII	289–294
Discovery II	1931	V	693, 696, 699
Meteor	1925	I	II
		IV	Probestation
	1926	X–XI	212–220
	1927	II	258–269
		III	270–290
		IV–V	291–292, 294–310
Michael Sars	1910	V	34–35, 38, 39A, 40, 44, 46
		VI	49C
Möwe	1911	VI–VII	12–26

The six σ_t-surfaces used in the present study are those for $\sigma_t = 24$, 25, 25.5, 26, 26.5 27. They all lie above the principal O_2-minimum, and are hence included within the troposphere.

Instead of the representation of identifying properties against σ_t as used by Parr (1938a, p. 136), the basis of the interpolations involved was the representation of the observed values on characteristic diagrams. On these a smooth curve was drawn for each station, which in most cases passed through each observed point. Where the serial observations are not closely spaced, there may be considerable latitude in drawing the smooth curves. For a few stations, after the interpolated values had been plotted on the preliminary draft of the isentropic charts and found in disagreement with nearby

stations, it was found advisable to redraw the characteristic curves so as to give interpolated values in better agreement.

The temperature-salinity diagrams were plotted in the form shown in Figure 8 below, the scale being 5° corresponding to 1 °/₀₀. A table was prepared giving the salinities for each degree of temperature and for $\sigma_t = 24$, 25, 25.5, etc, so that enough of each σ_t-line could be easily drawn on the t-S-diagram to intersect the t-S-curve. The values of temperature and salinity for each σ_t-surface were thus read off at these intersections.

The depths corresponding to the interpolated temperatures were obtained from temperature-depth curves. The scale was usually 2° corresponding to 100 meters.

The first characteristic diagram for oxygen was, I believe, that drawn by Jacobsen (1929, Fig. 15), which represented percentage saturation against salinity. Since percentage saturation depends on temperature and salinity as well as on oxygen content, however, it is not suitable for use as a characteristic diagram. Specific oxygen content has been plotted against salinity by Wüst (1935, Abb. 17 etc.), Rossby (1936, Fig. 16, etc.) and Seiwell (1937a, Fig. 8), and against temperature by Dietrich (1937, Abb. 2, 40 etc.). The last representation appears preferable, because temperature at most stations decreases downwards at all depths so that the diagram is more readily interpreted in terms of the vertical oxygen distribution. t-O_2-diagrams have been used here, in the same form and scale as used by Dietrich.

Where σ_t at an observed depth differed by 0.01 or less from one of the chosen σ_t-surfaces, the values observed at this depth were used without interpolation.

There being a unique relationship between temperature and salinity for a given σ_t-surface, representation of both would be redundant. The preference between the two lies with salinity,[4] because absolute values of salinity have an obvious significance, whereas absolute values of temperature are difficult to interpret due to the relatively strong vertical temperature gradient. This is especially true of a σ_t-surface lying within the layer of maximum salinity. For the isentropic analyses presented below, charts for depth, salinity and oxygen (in cc.l.$^{-1}$) have been prepared for each σ_t-surface.

For finding salinities at the intersections of the σ_t-surfaces with the sea surface, Böhnecke's (1936) atlas serves admirably. This gives on separate charts the mean distributions of salinity and density at the sea surface for the year and for each quarter over the whole Atlantic, and for each month over the North Atlantic. Figure 5 is a superposition of his yearly mean charts of salinity and density. Use is made below of quarterly values also; these were determined by copying the density lines on tracing paper and superposing the latter on the corresponding salinity charts.

V. DYNAMIC CALCULATIONS

While the principal tool to be used in deducing the circulation of the southern North Atlantic is isentropic analysis, it is also desirable to make some use of the computed gradient currents, both to add further information and to reveal discrepancies between the results of the two methods. Since for this region no dynamic calculations have been published except Jacobsen's (1929) charts, which are based on a very sparse network of

[4] Parr's (1938b, p. 13) argument in favor of temperature, that its interpolated values are more certain than those of salinity, is untenable in view of the unique relationship between the two on a σ_t-surface.

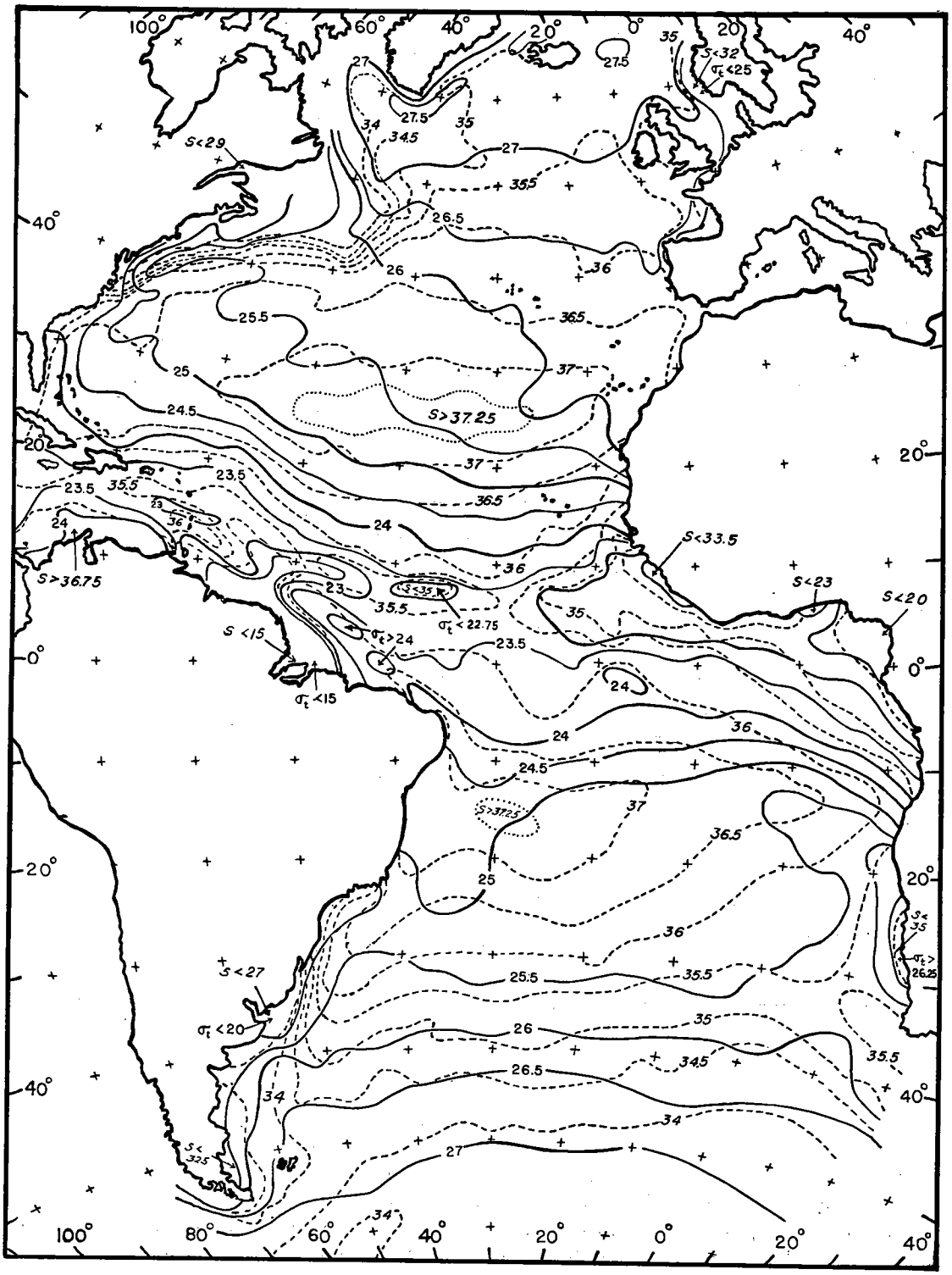

FIG. 5.—Surface density (σ_t, full lines) and salinity (broken lines) in the Atlantic Ocean, based on Böhnecke's (1936) atlas.

stations, it is therefore well to insert at this point the calculations for the *Atlantis* section along the fortieth meridian, stations 1161–1177. Temperature, salinity and σ_t profiles for this section have been presented by Iselin (1936, Figs. 32–34).

The topographies of the 0, 25, 50, 75, 100, 150, 200, 300, 400, 500, 750, 1000, 1500,

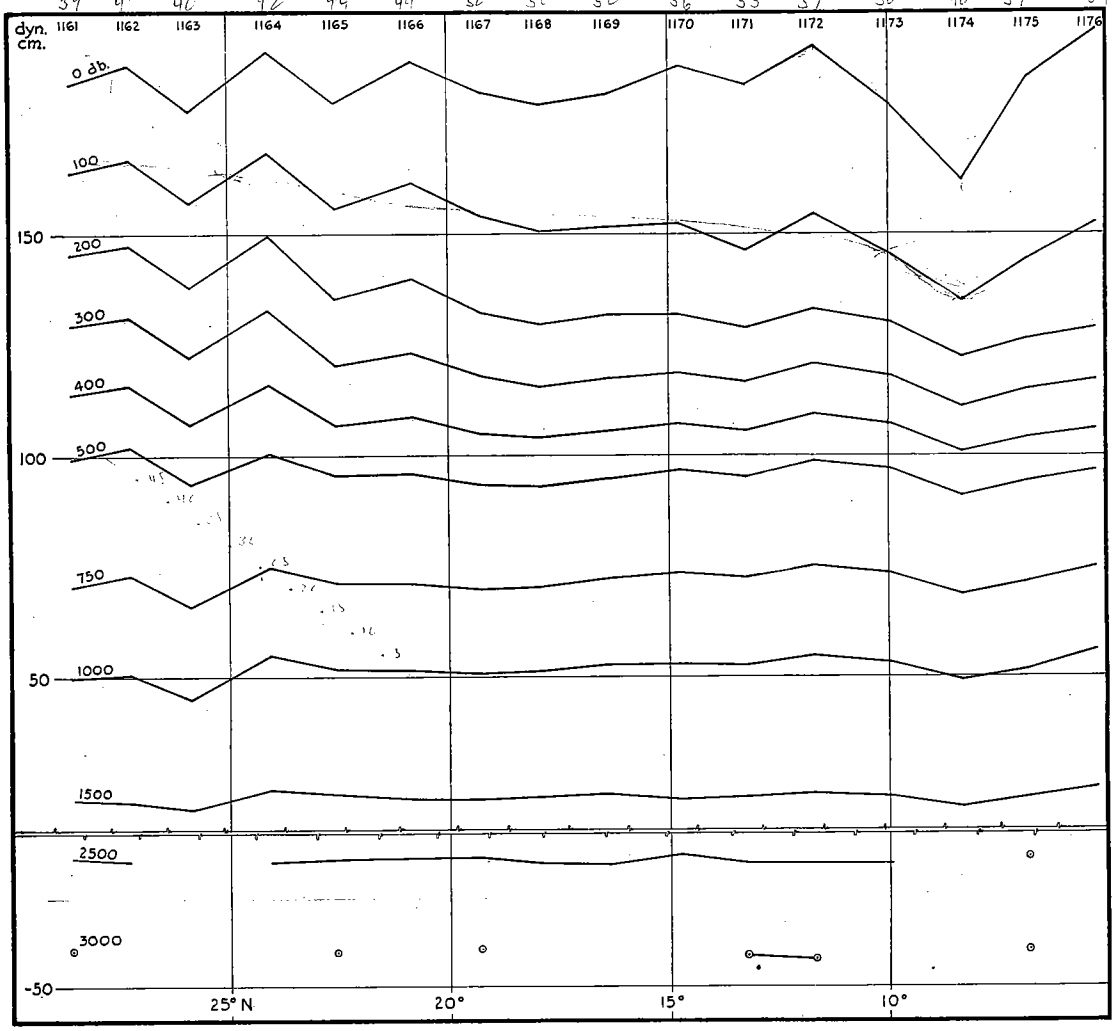

FIG. 6.—Topography of isobaric surfaces along *Atlantis* mid-Atlantic section. 2000 db. surface assumed level. Units are anomaly of dynamic height in dynamic centimeters. Station 1177 omitted because its serial observations extend to only 1183 meters.

2500, 3000, etc. decibar surfaces were computed, assuming the 2000 db. surface to be horizontal. The results for some of these are shown in Figure 6.

The topography of the sea surface indicates a strong west current between stations 1172 and 1174 (the North Equatorial Current) and a strong east current between 1174 and 1176 (the Equatorial Counter Current), both of which decrease rapidly down to 200 meters and then more slowly down to 2000 meters. North of station 1172 the topog-

raphy of the sea surface is irregular; at least some of this irregularity appears to be the fictitious result of internal waves. At intermediate depths, especially the 100, 200, and 300 db. surfaces, there is a general downward trend from station 1164 to station 1174, indicating a broad and relatively slow west current at these depths (also the North Equatorial Current). This general trend disappears at about 750 meters. The northern boundary of this current coincides with that of the trades: "at the time the *Atlantis* observations in mid-ocean were made, the horse-latitude belt was encountered between latitudes 23° and 26°N." (Iselin, 1936, p. 84).

On the general trend just mentioned are superimposed irregularities, which are probably due to internal waves. As Dietrich (1937, p. 519) has pointed out, these irregularities may often be reduced without losing the permanent features, by using a higher reference level. In the present case the 1000 db. surface may be assumed horizontal without affecting the permanent features except perhaps in reducing slightly the velocities on both sides of station 1174, and has been used as the reference level in computing the velocities shown in Figure 7. This figure was constructed by plotting the computed

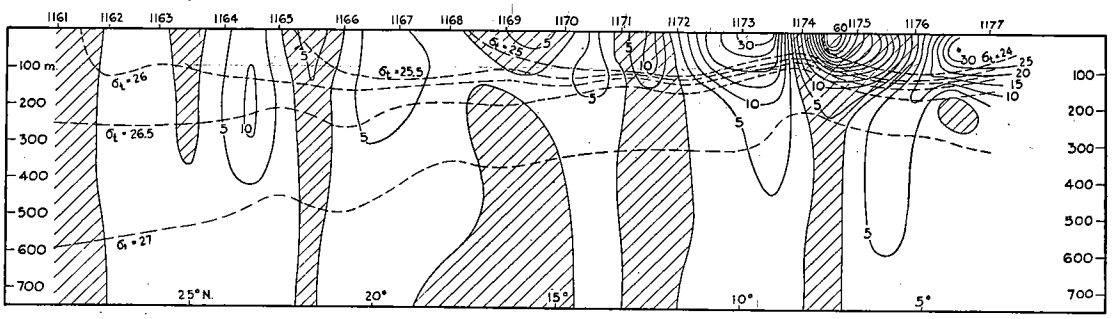

FIG. 7.—Longitudinal component of velocity computed for *Atlantis* mid-Atlantic section. 1000 db. surface assumed level. Lines for every 5 cm.sec.$^{-1}$, east currents hatched.

velocities along the vertical midway between each pair of stations, and drawing the equal velocity lines roughly according to linear interpolation between the plotted velocities. As is common with such representations of dynamic calculations, this procedure diminishes the areas of extreme velocities because the plotted velocities actually represent the average velocity between adjacent stations. Since, however, some of the maxima in this diagram appear fictitious, the procedure seems justifiable in this case. The intersections of the six σ_t-surfaces with this section are indicated by broken lines in the figure.

The general features of Figure 7 are in agreement with the navigational record of *Atlantis*. Quoting from Iselin again (1936, p. 52): "While crossing the trade wind belt the . . . record showed westerly currents varying between 8 and 20 miles per day. These conditions persisted as far south as station 1174 (Lat. 8°20'N.). Then in a few hours 12 miles of easterly set was experienced and strong tide rips were seen at the surface. . . . South of station 1176 a westerly current was again encountered." The computed velocities in the North Equatorial Current (maximum 30 cm.sec.$^{-1}$ or 14 miles per day between stations 1173 and 1174) are less than the observed ones; since the surface current is partly drift current, this is to be expected. The computed velocities in the Counter Current (maximum 65 cm.sec.$^{-1}$ between 1174 and 1175) apparently also agree with the very strong surface current observed there.

Iselin (1936, p. 86) has suggested that there is a shallow and weak surface counter (east) current between stations 1169 and 1170, or at about 15°N. He points out that, while the surface hundred meters is nearly homogeneous meridionally with regard to temperature, this current coincides with a sharp salinity gradient separating salt water to the north (>37.0 °/₀₀) from fresh water to the south (<36.4 °/₀₀). He suggests that this current is a result of the density distribution, or in other words that it is of thermal origin. Figure 7 clearly shows this shallow current of 125 meters depth, with surface velocity of 9 cm.sec.$^{-1}$

The two counter currents indicated in Figure 7 at latitudes of approximately 12½°N. and 22°N. appear most likely to be the fictitious result of internal waves. It would be hasty, however, to state definitely that such is the case, for they might represent eddies of a temporary nature. There is some reason to believe that the east currents at 25°N. and 28°N. are real, because at the time the section was made the trades did not extend this far north.

Mention should be made of the method of interpolation used in deriving dynamic heights at standard pressures. First the anomaly of dynamic thickness between each successive observed pressure (depth) was obtained. These were successively added from the top, giving the anomaly of dynamic depth for each observed pressure. The resulting values for a given station were plotted against pressure (1 dyn. cm. corresponding to 10 db.), and a smooth curve drawn. The resulting curve is always regular, usually having no points of inflection, and may be drawn very accurately without difficulty. From this curve the anomaly of dynamic depth may be taken for standard pressures, including the reference level (and also at the pressure for a given σ_t-surface). The anomalies of dynamic height are then obtained by subtracting the anomalies of dynamic depth from the anomaly of dynamic depth at the reference level.

As mentioned in Chapter III, a method has been recently suggested for representing gradient flow on isentropic charts (Montgomery, 1937). Since this method has not yet been put into practice, it seemed advisable to test it in connection with the dynamic calculations above. This trial was made not for a surface, but merely for the intersection of the $\sigma_t = 27$-surface with this section for which the dynamic calculations were already available.

Using axes with x directed $\pi/2$ *cum sole* from y, the expression derived for gradient flow in a σ_t-surface was

$$v = \frac{1}{f}\left(\frac{\mathrm{d}(\Phi_a + \alpha_a p)}{\mathrm{d}x}\right)_A .$$

f is the Coriolis parameter, Φ_a the anomaly of dynamic height, p the pressure, and the subscript A indicates that the differentiation is carried out along the σ_t-surface. This simplified form of the equation was derived from the exact form by assuming that the anomaly of specific volume, α_a, is constant over the σ_t-surface. The advantage of this form of the gradient current equation lies in the fact that the current in the surface is derived from the variation of a single quantity, $(\Phi_a + \alpha_a p)$. It is proposed to call this "geostrophic potential."[5]

The equation above is in standard metric units. Let H_i represent the geostrophic

[5] This is in accord with the term "geostrophic wind," designating the velocity such that the existing horizontal pressure gradient is exactly balanced by the fictitious deflecting force on unit volume due to the earth's rotation.

potential in the practical unit of dyn. cm. If L represents latitude and M is distance in nautical miles, the velocity in cm.sec.$^{-1}$ is

$$v = \frac{37}{\sin L} \frac{\Delta H_i}{\Delta M}.$$

In Table 3, $V_a = 10^5 \alpha_a$, and H_a is the ordinary anomaly of dynamic height in dyn. cm. (obtained from the interpolation curve for each station mentioned three paragraphs above). Hence $H_i = H_a + V_a P \cdot 10^{-3}$.

The quantity V_a as listed in Table 3 for *Atlantis* stations 1161–1177 at the $\sigma_t = 27$-surface is seen to be not constant, as was assumed in deriving the gradient current equation. However, the difference between successive stations is not more than 2 units in V_a (except in one case where it is 3), which is within the possible error in determining V_a from Bjerknes' (1912) tables, so the method appears to be permissible. The table shows the complete calculation carried out and presents the resulting velocities. The x-coordinate is chosen northward, so v is positive westward.

TABLE 3

VELOCITY CALCULATIONS FOR $\sigma_t = 27$-SURFACE, ASSUMING 1000 DB. SURFACE HORIZONTAL

Atlantis	P	V_a	H_a	$V_a P \cdot 10^{-3}$	H_i	$\frac{37}{\Delta M \sin L}$	v	Fig. 3
1161	590	124	37.9	73.2	111.1			
						.95	−1.3	−2.0
1162	570	123	42.4	70.1	112.5			
						1.01	+3.2	+2.8
1163	540	122	43.4	65.9	109.3			
						.82	+2.5	+2.0
1164	507	121	45.0	61.3	106.3			
						1.03	+3.1	+3.2
1165	445	120	49.9	53.4	103.3			
						.95	−1.4	−1.1
1166	485	121	46.1	58.7	104.8			
						1.16	+3.5	+2.6
1167	416	119	52.3	49.5	101.8			
						1.41	+3.8	+2.2
1168	350	116	58.5	40.6	99.1			
						1.35	−0.3	+0.1
1169	368	117	56.3	43.0	99.3			
						1.45	−1.3	−2.3
1170	337	115	61.4	38.8	100.2			
						1.66	+3.3	+2.7
1171	320	114	61.7	36.5	98.2			
						1.87	−3.7	−3.4
1172	318	114	63.9	36.3	100.2			
						1.86	+2.2	+2.1
1173	305	113	64.5	34.5	99.0			
						2.40	+9.4	+8.3
1174	210	111	71.8	23.3	95.1			
						3.12	−4.4	−5.1
1175	253	112	68.2	28.3	96.5			
						3.73	+7.8	+7.6
1176	272	112	63.9	30.5	94.4			
						4.07	−0.4	+1.0
1177	312	113	59.3	35.2	94.5			

These velocities may be compared with those interpolated from the values used in constructing Figure 7; the interpolated values are listed in the last column of the table. The results are in sufficiently close agreement to show the practicability of this new

application of the gradient current equation. Better agreement may be obtained by using a constant average value of V_a, in this case 117, in computing $V_a P \cdot 10^{-3}$.

Since a variation of α_a (or V_a) along a σ_t-surface can occur only under fairly high pressures, it can be concluded that for surfaces higher than the $\sigma_t = 27$-surface the variation would be less than found in the example above. Hence this method, involving the assumption regarding the constancy of α_a, appears applicable at least for σ_t-surfaces not deeper than $\sigma_t = 27$.

As with any other application of dynamic calculations to instantaneous observations, internal waves exert a large disturbing influence. It is to be expected that only the major features of the velocity distribution computed by this method are of significance.

VI. $\sigma_t = 27$-SURFACE (CHARTS 2–4)

In the following small table are presented for ready reference the minimum salinity which can occur at this surface, taken from Krümmel's (1907, p. 235) "Tabelle für das Dichtigkeits maximum des Seewassers," and corresponding values of salinity and temperature:

33.50 (min.)	33.60	34.00	34.50	35.00	35.50	36.00 °/₀₀
−3.21°	0.00°	4.1°	7.4°	9.8°	12.0°	13.8°

The station values of depth, salinity and O_2-content, which have been plotted on Charts 2, 3, 4, form the basic data for the analysis of the flow on this surface. The depth of the surface within the region of study ranges between 200 and 840 meters. Salinity ranges between 34.76 and 35.91 °/₀₀ (except *Atlantis* 1201 which shows 35.98 °/₀₀), temperature between 8.25° and 13.56°, and O_2-content between 0.61 and 4.78 cc.l.$^{-1}$

With a few exceptions (*Dana* 1162, 1164; *Meteor* 267, 268; *Möwe* 24, 25) salinity increases upward at this surface. At most stations, furthermore, it occurs within the lower part of the nearly straight portion, i.e. near the inflection point, of the t-S-curve between the tropospheric S-maximum and the S-minimum of the subantarctic intermediate water (Wüst, 1935, p. 111).

According to Figure 5 this σ_t-surface reaches the sea surface north of 50°N. at salinities of 33.6–35.6 °/₀₀, and between 50°S. and 58°S. at 33.9–34.1 °/₀₀. This indicates at once that high salinities can originate only in the North Atlantic, while there is a larger source region for low salinities in the South Atlantic. The Pacific and Indian Oceans are left out of consideration, which may not be justifiable since this surface extends continuously into these oceans from the South Atlantic (in all seasons).

The following small table of quarterly values of salinity at the intersection with the sea surface has been derived from Böhnecke's (1936) atlas:

Season	North Atlantic		South Atlantic	
Year	north of 50°N.	33.6–35.6 °/₀₀	50°–58°S.	33.9–34.1 °/₀₀
D–F	40°–70°	33.0–36.3	south of 48°	33.5–34.2
M–M	north of 42°	33.0–36.2	51°–59°	33.5–34.3
J–A	north of 54°	33.5–35.3	42°–57°	33.8–35.0
S–N	north of 54°	32.0–35.5	42°–57°	33.7–34.6
Total range		32.0–36.3		33.5–35.0

In this way the total range in salinity at each source region is increased over that found from the yearly mean charts, and probably (though not necessarily) the range would be further increased by taking it directly from the original surface observations. The total

ranges found above, however, may be assumed to represent the extreme salinity limits for water that originates in appreciable quantities at these sources. Since the minimum salinity which can occur at $\sigma_t = 27$ is 33.50 °/₀₀, the values less than this are due to slight inconsistencies in the corresponding charts of density and salinity. It may be concluded, then, that water of salinity greater than 35.0 °/₀₀ originates only in the North Atlantic, while water of salinity between 33.5 and 35.0 °/₀₀ can originate in either ocean.

There is one notable region, outside the Straits of Gibraltar, where it is known that water masses of different density mix in quantities which assume important magnitude, and hence the source regions for the σ_t-surfaces are not limited to their intersections with the sea surface. The deep water of the Mediterranean which flows out through the Straits is originally at about $\sigma_t = 29.0$ (for instance *Michael Sars* 18 and 19, which are 20 and 70 miles inside the Straits; the sill depth is about 210 meters), yet in the Atlantic except in the immediate vicinity of Gibraltar no water is found exceeding $\sigma_t = 28.0$. The Mediterranean water is, in fact, completely mixed with Atlantic water during its outflow along the bottom before it can reach its own density level. The admixture of this salt Mediterranean water accounts for a marked enrichment of some layers of the Atlantic, especially of the upper North Atlantic deep water (Wüst, 1935, p. 127) which is characterized by a salinity maximum at about $\sigma_t = 27.8$. The question arises as to whether the water of the $\sigma_t = 27$-surface is enriched by the Mediterranean outflow. Since this cannot be definitely answered except by a study of the salinity distribution on the $\sigma_t = 27$-surface in the region immediately west of the Straits of Gibraltar, the answer will not be attempted here. The fact that the highest salinity for the region studied occurs in the vicinity of the Canary Islands, however, suggests that the Mediterranean outflow may exert some influence.

Of course the analysis of any σ_t-surface cannot be complete so long as arbitrary boundaries are imposed on the region studied. The entire surface between its northern and southern natural limits, or as much of it as is feasible in view of seasonal fluctuations, must be analyzed before the exact origin of the various water types can be determined. In the present case this is precluded by practical limitations. The information above from sea surface conditions partly fills this lacuna.

Turning to Chart 2, certain broad features of the circulation in the $\sigma_t = 27$-surface may be tentatively deduced from its topography. Throughout most of the region north of 15°N. there is a fairly uniform downward slope in a direction slightly west of north, which indicates a uniform current running slightly south of west. The deepest region is found midway between Bermuda and the Bahamas; this depression or trough calls for an anticyclonic circulation around it. Centered at about 8°N. 42°W. is a pronounced dome which calls for a cyclonic circulation. Along the coast of South America the σ_t-surface appears to be at a high elevation, with a trough further offshore; along the intervening slope one would expect to find a current northwest in sense. Finally the elevation appears to be high along the African coast between 20°N. and 30°N., corresponding to a southerly current.

The salinity distribution on Chart 3 corroborates these results and adds much new information. The lowest values are 34.67 °/₀₀ (*Meteor* 297) and 34.70 °/₀₀ (*Atlantis* 1181) near the equator at 45°W., and 34.72 °/₀₀ (*Deutschland* Reihe 25) and 34.73 °/₀₀ (*Meteor* 212) near the equator at 30°W. Both of these regions clearly represent axes of flow from the intersection with the sea surface in the South Atlantic, for they are completely cut off from the North Atlantic intersection by higher salinities. The wide

hatching covers the area of $S < 35$ °/₀₀, which is the highest salinity at the South Atlantic intersection in any quarter of the year. From the region at 45°W. a tongue of fresh[6] water with increasing minimum values extends northwest; this can only be interpreted as the axis of a flow northwestward, the minimum salinity being gradually increased, supposedly by lateral mixing. This axis crosses five sections (*Atlantis*, *Meteor*, *Dana*, *Meteor*, *Atlantis*) each of which shows the minimum salinity, so it is clearly marked and evidently permanent. It is concluded in the same way that from the region at 30°W. one current axis extends northwest (shown by minimum salinities as it crosses two *Meteor* sections at stations 260 and 303 and the mid-Atlantic *Atlantis* section at station 1173), and another northeast to 20°N. near the African coast probably with offshoots at 8°N. and 15°N. This northeast current axis, although its course is poorly defined except where it crosses the *Möwe* section at station 20, appears to be of considerable importance as the chief agent for supplying fresh water to the region studied.

The highest salinities are 35.91 °/₀₀ (*Meteor* II) and 35.88 °/₀₀ (*Michael Sars* 34) near the Canary Islands. From here there appears to be a salt tongue extending southward along the African coast at least to 11°N.; it is indicated clearly only at the eastern end of the *Möwe* (station 22) and *Meteor* (station 269) sections. The three western *Atlantis* sections all show salinity maxima (stations 2729, 1210, 1475) decreasing toward the west; this well marked west flow can probably be traced from the general vicinity of the Canary Islands, although it is not indicated at the mid-Atlantic *Atlantis* section. Hence it appears as a continuous flow of salt water crossing nearly the whole Atlantic north of 22°N. The slight maximum on this axis between 45°W. and 60°W. is not necessarily indicative of vertical mixing or non-isentropic flow, and may rather reflect fluctuations in the salinity of the tongue. The interpretation suggested is that this flow enters across the 30th parallel at about 23°W. and gained its salt at the North Atlantic intersection with the sea surface, and that it is separated by slightly fresher water (based on *Michael Sars* 44, 46, 49 C) from the salt south flow along the African coast which has been slightly enriched by Mediterranean outflow; but an extension of the chart northward might easily disprove this. There is indication of a fresh current with anticyclonic curvature between Bermuda and the Bahamas.

The very high salinities recorded at *Atlantis* 1200 and 1201 near the South American coast call for special discussion. These cannot be due to advection along the $\sigma_t = 27$-surface, and could have been produced only by local vertical mixing aided by the stirring action of the continental shelf. Above in this vicinity there is a little very salt water of North Atlantic origin (see $\sigma_t = 25.5$-surface salinity distribution) with the following observed characteristics:

Station	P	t	S	σ_t
Atlantis 1200	99	21.67°	36.69 °/₀₀	25.61
1202	101	21.38°	37.05	25.97

Below there is the salt upper North Atlantic deep water, which has been observed in the vicinity at the following points:

Station	P	t	S	σ_t
Atlantis 1202	1009	4.86°	35.01 °/₀₀	27.72
1203	1335	4.37°	34.99	27.77
2748	1060	4.92°	34.96	27.68
	1460	3.82°	34.97	27.80
Meteor 290	1590	4.35°	34.98	27.75
291	1380	4.59°	34.97	27.72

[6] Throughout the text the abbreviations "fresh" and "salt" mean "relatively fresh" and "relatively salt."

The very salt water on the $\sigma_t = 27$-surface could have been formed by mixture of these two water types in nearly pure form. The t-S-diagram illustrating the water masses concerned is given in Figure 8. It seems unlikely, however, that the upper water mass,

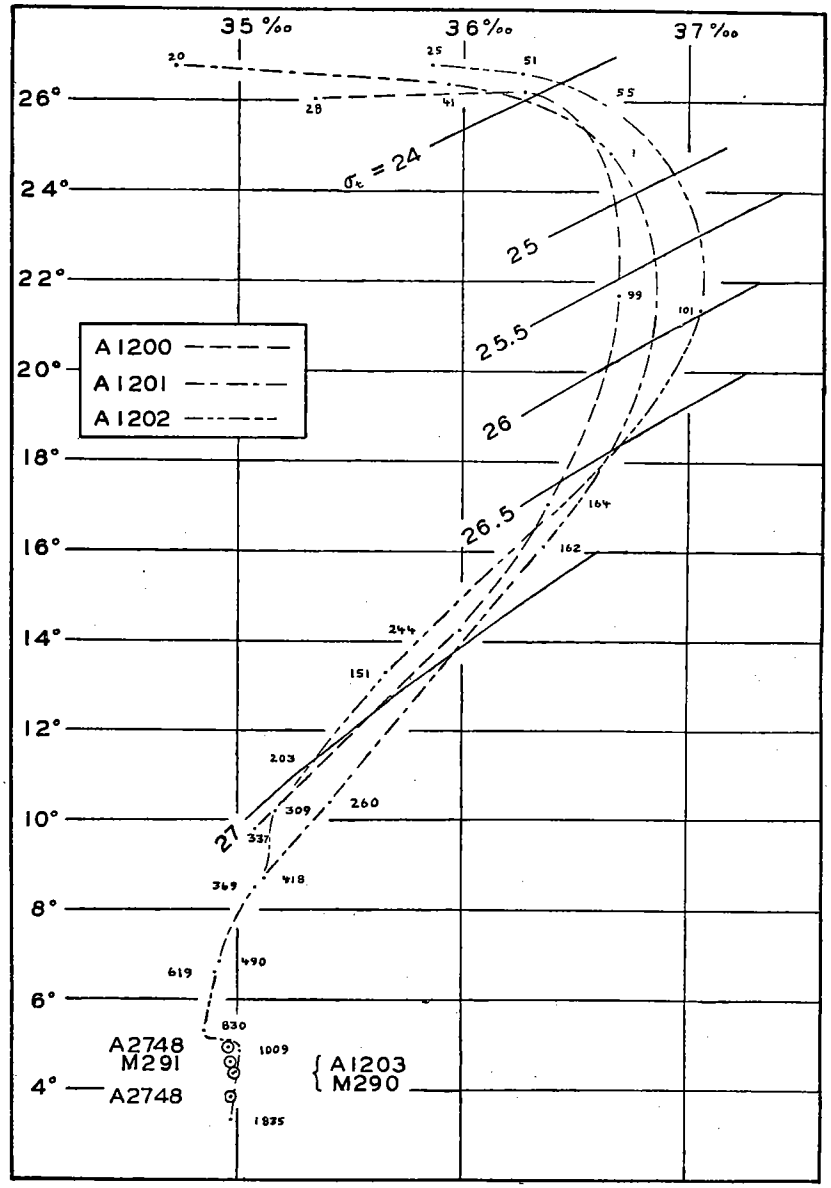

FIG. 8.—t-S-diagram for conditions in vicinity of *Atlantis* stations 1200 and 1201. Small numbers are depths in meters.

which is present in such small amount, should mix in appreciable quantity with the lower water mass of such different density, especially without strong admixture of the intervening fresher water (subantarctic intermediate water). It appears more likely that

the observations are in error, especially for *Atlantis* 1201 at 162 and 260 meters. There is some reason for expecting this, because these *Atlantis* stations were made in a swift surface current, and due to large wire angles the water bottles may not have functioned properly. This conclusion regarding the accuracy of the observations is based fundamentally on the representation of salinity on a σ_t-surface, and serves as an incidental example of the strength of this method of representation.

No attention has been paid to the large variations in salinity recorded along the short *Discovery* section.

Turning to Chart 4, it is found that further information may be derived from the oxygen distribution. The lowest value, 0.61 cc.l.$^{-1}$, is found at 10°N. 27°W.; this region of low values appears completely surrounded by higher values so it must be concluded (on the basis of the working hypothesis) that oxygen is consumed here. This is corroborated by a manuscript chart prepared by Professor Iselin showing the distribution of the O_2-minimum regardless of depth; values less than 1.20 cc.l.$^{-1}$ are limited to a band extending from 11°N. 28°W. to the African coast. It is seen that the currents of low salinity entering across the equator are characterized by relatively rich O_2-content, 2.70–3.90 cc.l.$^{-1}$ The one along the South American coast continues as a rich tongue evident in each of the five sections it crosses; the one moving northeast toward Africa, however, loses its oxygen by consumption and lateral mixing while passing through the region poor in oxygen and merges as an O_2-poor tongue. The *Atlantis* mid-Atlantic section shows a distinctly low O_2-value at 15°N. This may be due to local O_2-consumption, but is here interpreted as coming from the region of lowest oxygen by a route coinciding with the offshoot from the main northeast current axis of low salinity; it thus crosses the *Meteor* section at its lowest value of 1.37 cc.l.$^{-1}$ at the Cape Verde Islands (station 309). Professor Iselin's chart also shows an O_2-poor tongue extending westward in this region.

The richest water, 4.78 cc.l.$^{-1}$ (*Meteor* II), is found near the Canary Islands coinciding with the saltest water. The slight maximum of 4.08 cc.l.$^{-1}$ in the mid-Atlantic *Atlantis* section (station 1164) is interpreted as coming from there and hence helps to locate the salt axis crossing the ocean north of 22°N. Another flow rich in oxygen is indicated as entering from the north at 45°W.

Identical arrows have been drawn on the three charts. These represent primarily the axes of tongues of salt or fresh water or of water rich or poor in oxygen. Some of them, especially the fresh tongues from south of the equator and the salt tongue along the African coast, represent current axes also. Arrows with broken shafts represent trajectories of temporary or intermittent nature or those whose existence is more doubtful. Hence it is permissible that a broken arrow cross another arrow. The contour lines, S-lines and O_2-lines have been drawn to agree with the observations, and also to agree with the interpretation indicated by the arrows.

The cyclonic eddy centered at about 8°N. 42°W. demands individual attention. The fresh and rich north flow on its east side and west flow on its north side, and the O_2-poor westward flow further north have been mentioned. The topography of the σ_t-surface calls for a closed cyclonic circulation, hence it appears most likely that the high salinity of 35.06 $^{o}/_{oo}$ at 2°N. 41°W. (*Atlantis* 1178) has come from the north around the west side of the eddy, and this axis of motion may be drawn as a continuation of the O_2-poor axis on the north side. Since both the *Dana* (station 1172) and *Meteor* (station 298) sections show S-maxima coinciding with this axis, it appears to be a permanent feature. The other arrows in the eddy are drawn to explain details of the salinity and oxygen distributions

along the various sections; they are not to be regarded as permanent features of the eddy.

As drawn, each of the arrows in the eddy has a component toward the center, which indicates horizontal convergence. In a steady state this would necessitate vertical motion through σ_t-surfaces. It is more compatible with the working hypothesis, however, that there is intermittent discharge from the eddy, probably toward the east.

A current axis can be discerned from the distribution of salt and oxygen only if the water in the current shows a maximum or minimum of one or both of these substances with respect to the surroundings. In the present case, on the basis of the topography of the σ_t-surface, it appears that the main stream is a general west current (North Equatorial Current) covering most of the zone between 8°N. and the northern limit of the chart. The dynamic calculations for the mid-Atlantic *Atlantis* section should serve to give the order of magnitude of the speed of this current. In order to eliminate the apparently fictitious effect of internal waves, it is best to find the average across the whole current. The average between 8°N. and 29°N. from the last column of Table 3 (between stations 1162 and 1174, regarding them as equally spaced) is 1.7 cm.sec.$^{-1}$ The supply of water to this current in the east is salt water from the north and fresh water from the south, so the current is characterized by a cross-stream salinity gradient. The arrows on the eastern side of the charts have been drawn with the view in mind that this main stream must be supplied by water from the north and south. In the west, although the arrows show the main stream as passing only to the north of the Antilles, it is probable that part of it enters the Caribbean as indicated by the topography of the σ_t-surface.

In this regard Parr's (1938b, Figure 15) larger scale synoptic chart for January 1937 of temperature on the $\sigma_t = 27$-surface in the eastern Caribbean is useful as a westward extension of the region studied. It shows a tongue of water warmer than 12.6° (>35.67 °/$_{oo}$) entering the Caribbean (at 17°N.) between Montserrat and Guadeloupe. From the general continuity of salinity across the chain of Lesser Antilles it appears likely that there is flow across this chain all along its length. From the greater contrasts in salinity on the east side than on the west side of the islands, the flow must be westward. A single station (*Atlantis* 2735) just north of the warm, salt tongue mentioned and one (*Atlantis* 2770) just south of it show temperatures colder than 11.0° (<35.27 °/$_{oo}$); these "pools" (which do not appear on the $\sigma_t = 26.5$-surface, Parr, 1938b, Figure 14) so far north of the main body of cold, fresh water remain unexplained (Parr, 1938b, pp. 10–11).

The fresh current along the South American coast shown on Chart 3 appears from Parr's chart to extend, although not continuously, into the Caribbean as far west as 67°W., where water colder than 10.6° (<35.18 °/$_{oo}$) was encountered (*Atlantis* 2801, 2802). Except for this fresh current entering the Caribbean near the South American coast, which is South Atlantic water already mixed with salter North Atlantic water, all the water passing through the Lesser Antilles, since its salinity is well above the maximum of 35.0 °/$_{oo}$ for South Atlantic water, is of North Atlantic origin. This agrees with Parr's (1938b, p. 9) conclusion that for *Atlantis* stations 2736–2741 "the layers between maximum salinity and the isothermal surface of about 12°C. [ca. $\sigma_t = 27$] are entirely of Sargasso Sea type" (though of course their origin at the sea surface is far north of the Sargasso Sea).

The analysis of the charts, as represented by the arrows and the additional concept of the main west stream, forms a consistent picture in itself. It is not necessary to consider vertical mixing or flow through σ_t-surfaces in order to explain the hydrographic data on the $\sigma_t = 27$-surface.

VII. $\sigma_t = 26.5$-SURFACE (CHARTS 5–7)

32.89 (min.)	32.98	33.50	34.00	34.50	35.00	35.50	36.00	36.50	37.00 °/₀₀
−3.09°	0.00°	5.1°	8.1°	10.4°	12.6°	14.4°	16.2°	17.7°	19.3°

The depth of the surface ranges between 90 and 500 meters, except in the northeast corner of the region of study where a number of stations show it at a shallower depth and one (*Meteor* II) shows $\sigma_t = 26.5$ at the sea surface. Salinity ranges between 35.16 and 36.86 °/₀₀, temperature between 13.15° and 18.85° and O_2-content between 1.35 and 5.67 cc.l.$^{-1}$ With a few exceptions (*Michael Sars* 34, 35, 38, 39A, 40, 44, 49C; *Möwe* 15, 21) salinity increases upward at this surface also, which occurs as a rule in the middle or upper part of the straight portion of the *t-S*-curve between the tropospheric S-maximum and the S-minimum of the subantarctic intermediate water.

Böhnecke's atlas gives the following ranges of salinity for the intersections of the $\sigma_t = 26.5$-surface with the sea surface:

Season	North Atlantic		South Atlantic	
Year	north of 40°N.	33.0–36.1 °/₀₀	42°–56°S.	33.5–34.8 °/₀₀
D–F	north of 26°	32.8–37.0	44°–58°	33.7–34.5
M–M	north of 23°	32.8–37.2	44°–56°	33.5–34.4
J–A	north of 49°	32.0–35.6	35°–56°	33.3–36.2
S–N	north of 47°	32.0–35.8	36°–56°	33.5–35.6
Total range		32.0–37.2		33.3–36.2

While this surface is continuous from the South Atlantic into the Indian Ocean in all seasons, it is closed to the Pacific in the quarters J–A and S–N. It can be said definitely that, for this surface, the high salinitites of about 36.8 °/₀₀ found in the vicinity of the Canary Islands are not due to Mediterranean outflow. For, north of 25°N. the S-maximum occurs at the sea surface (see Fig. 3), while salinity at the sea surface west of the Straits of Gibraltar is <36.5 °/₀₀ (see Fig. 5; also Böhnecke's monthly charts show <36.5 °/₀₀ except in October and November, the charts for these two months showing <36.75 °/₀₀).

Along the African coast as far south as 16°N. surface densities are greater than $\sigma_t = 26$ (see Chart 8). Along a coastline vertical mixing is to be expected between surface water and sub-surface water of not too greater density, and this may be accompanied by non-isentropic flow. Since there is horizontal divergence of surface water along this part of the African coastline (Montgomery, 1936, Fig. 1), it is probable that part of the compensating convergence occurs at about the $\sigma_t = 26.5$-surface. Hence it may be expected that the coastline north of about 16°N. is a sink for this surface.

While this applies for most of the year, in late winter the $\sigma_t = 26.5$-surface does not reach to the coastline north of 16°N. The most southern extension of the $\sigma_t = 26.5$-line at the sea surface occurs in March; Chart 5 shows its position in this month.

As in analyzing the charts for the $\sigma_t = 27$-surface, especial attention has been paid to contrasting values within each single oceanographic section, which more closely represents synoptic data. It is not necessary to discuss each of the arrows as in the preceding chapter, especially since there is a similarity in the flow patterns on the two surfaces.

A striking feature of the salinity distribution shown on Chart 6 is the crowding of the lines in a band extending from the African coast at 20°N. toward the west-southwest. Although this crowding is fictitiously accentuated because the band parallels the *Meteor* and *Dana* sections, its presence is nevertheless demonstrated where the band crosses three sections nearly perpendicularly (between *Möwe* 19 and 21, *Atlantis* 1171 and 1172,

Meteor 288 and 289). The band of strong salinity gradient is interpreted as coinciding with the axis of the North Equatorial Current, which is fed by salt water from the north and fresh water from the south. The interpretation is in disagreement with the results of the dynamic calculations for the mid-Atlantic *Atlantis* section, which give a counter current (5 cm.sec.$^{-1}$) between stations 1171 and 1172. Although this computed velocity is regarded as the fictitious effect of internal waves, the dynamic calculations may be utilized for a rough determination of the average velocity of the Equatorial Current across its whole width at this σ_t-surface. Considering it to extend from 10°N. to 25°N. (stations 1163 to 1173), the average velocity is 2.4 cm.sec.$^{-1}$ The isentropic analysis indicates that the Equatorical Current has a marked component equatorward.

Parr's (1938b, Figure 14) chart of temperature on this surface also serves as an extension of the region of study into the Caribbean. As on the deeper surface, the tongues indicate flow into the Caribbean all along the Lesser Antilles south of Montserrat. The warmest enters (at 15°N.) between Dominica and Martinique and carries water warmer than 17.6° (>36.47 °/₀₀) as far as 65°W. (*Atlantis* 2784), and the salt tongue shown on Chart 6 at 13°N. is found to extend to the same longitude with water warmer than 17.0° (>36.27 °/₀₀, *Atlantis* 2787 and 2788). The fresh tongue immediately south of the latter is colder than 16.6° (<36.13 °/₀₀) as far west as 67°W. (*Atlantis* 2797).

The large cyclonic eddy is confined to a narrower zone, and extends further west than on the $\sigma_t = 27$-surface. Again, while the arrows indicate horizontal convergence in the eddy and thus suggest vertical divergence, it appears probable that the eddy is not always closed so that it may discharge intermittently.

On this surface the agreement between adjacent stations of different cruises is far from close in a number of instances (*Carnegie* 30, 35.78 °/₀₀, *Dana* 1181, 36.29 °/₀₀; *Meteor* 286, 36.43 °/₀₀, *Deutschland* Reihe 20, 35.98 °/₀₀; *Challenger* 1326, 36.65 °/₀₀, 1564, 36.38 °/₀₀, etc.). This means either that the flow pattern is unsteady or that the amount of dissolved substances in the various tongues undergoes time fluctuations of considerable magnitude. Probably both are true and lend uncertainty to the flow pattern derived, especially in the northern part of the region. The analysis of the area in the northeast which is absent in late winter is necessarily subject to even more doubt; in any case it is not worthwhile to study this in detail because a close survey has recently been made on the *Meteor* of the waters off the African coast between 10°N. and 28°N. (Defant 1937, Abb. 2).

The course of the inflow of fresh water which supplies the Equatorial Current may also be designated as quite uncertain because it is indicated as flowing northeast through a region without observations between the two *Meteor* sections. There is, however, some evidence for the course chosen, as follows: (1) no salinity lower than 35.35 °/₀₀ is found at the southeasternmost *Meteor* section (also the deepest observation at station 219 is 189 meters, 35.38 °/₀₀, $\sigma_t = 26.48$) so the inflow does not appear to cross it north of the equator, (2) the σ_t-surface occurs considerably deeper along most of this section than at the next *Meteor* section, indicating a northeast flow between, (3) the lowest salinity on Chart 6 is 35.16 °/₀₀ at 5°N. 28°W. (*Deutschland* Reihe 25), and a low value is found at 5°N. 33°W. (*Meteor* 261) also, helping to locate the fresh tongue.

In spite of these uncertainties, two main features of the analysis stand out definitely: the course of the axis of the North Equatorial Current, and the presence, apparently permanent, of a large cyclonic eddy centered at about 9°N. 40°W. It is again possible, furthermore, to make a consistent analysis that does not require flow through σ_t-surfaces.

The circulation derived for this surface may be compared with that from Defant's analysis of the second maximum of the vertical temperature gradient. The latter circulation applies to layers above the $\sigma_t = 27$-surface (cf. p. 9) and, he says (1936, p. 334), to layers below the principal "Sprungschicht." The lower boundary of the "Sprungschicht" (Defant, 1936, Beilage XLI) is in places deeper than the $\sigma_t = 26.5$-surface (Chart 5), so the comparison should strictly be made with a surface intermediate between $\sigma_t = 26.5$ and $\sigma_t = 27$, but this difference is immaterial. His current arrows indicate (1) a current from the Gulf of Guinea passing southwest across the equator at 30°W., which is not evident on my charts, (2) a flow which coincides with the northeast fresh current from south of the equator, and (3) a southwest movement starting at 15°N. 30°W., which falls within the North Equatorial Current, and recurving southward at 40°W., which latter is in disagreement with my charts.

VIII. $\sigma_t = 26$-SURFACE (CHARTS 8–10)

32.27 (min.)	32.36	32.50	33.00	33.50	34.00	34.50	35.00	35.50	36.00	36.50	37.00	37.50 °/₀₀
−2.96°	0.00°	1.9°	6.0°	8.8°	11.1°	13.1°	15.0°	16.6°	18.2°	19.7°	21.1°	22.5°

The greatest depth of the surface is 265 meters. Salinity ranges between 35.50 and 37.19 °/₀₀, temperature between 16.65° and 21.73°, oxygen between 1.97 and 5.46 cc.l.$^{-1}$

This surface normally reaches to the sea surface within the region of study, the intersection being shown by the dotted line on each of the three charts (from Fig. 5). The intersections with this line of the sea-surface salinity lines, which are indicated on Chart 9, have been utilized in drawing the salinity lines on this chart.

As suggested at the end of Chapter III, it may be that equality exists between the convergence of the drift current in any locality and the strength of source for the σ_t-layer intersecting the sea surface there. Mean July atmospheric conditions over the Atlantic indicate fairly strong convergence of the drift current between 15°N. and 35°N. except near the American coast and more especially in the immediate vicinity of the African coast (Montgomery, 1936, Fig. 1); this general result may be expected to hold for all months of the year.[7] Hence the indications from surface conditions are that the intersection of the $\sigma_t = 26$-surface with the sea surface within the region studied is a source for the σ_t-surface except near the African coast where it is a sink.

Böhnecke's atlas gives the following ranges of salinity for the intersections of the $\sigma_t = 26$-surface with the sea surface:

Season	North Atlantic		South Atlantic	
Year	north of 22°N.	32.7–37.3 °/₀₀	36°–56°S.	33.0–35.4 °/₀₀
D–F	20°–58°	33.0–37.4	39°–56°	33.0–33.3
M–M	20°–60°	31.6–37.5	40°–55°	32.0–34.9
J–A	north of 30°	32.0–36.0	12°–55°	32.0–37.0
S–N	28°–73°	31.0–36.8	12°–55°	33.0–36.5
Total range		31.0–37.5		32.0–37.0

This surface is open to the Pacific Ocean in the quarter D–F only, and to the Indian Ocean in the quarters D–F and M–M only.

This surface occurs somewhat below the tropospheric S-maximum and, as mentioned in Chapter II, coincides very roughly with the surface of maximum vertical density

[7] A computation similar to this one for July has been made by Mr. E. M. Brooks for January, and indicates stronger convergence than in July, but limited to the zone between 15°N. and 30°N. approximately.

gradient. It occurs so near the sea surface that its contours cannot be expected to agree closely with the direction of the gradient current, as they did for the deeper surfaces (Parr, 1938a, pp. 136–137).

The most striking feature of this surface is again the zone of strong gradient of salinity and oxygen, bounded on the north by an axis of weak maxima of salinity and oxygen and on the south by strong minima of salinity and oxygen. This is interpreted as before, that the two axes and the intervening gradient constitute the North Equatorial Current. The strong part of this current at the fortieth meridian thus appears from the isentropic analysis to extend in width from 10°N. to 18°N.

TABLE 4

VELOCITIES ON $\sigma_t = 26$-SURFACE ALONG *ATLANTIS* MID-ATLANTIC SECTION FROM DYNAMIC CALCULATIONS, POSITIVE WESTWARD

STATION	L	P	v	
1162	27°15′N.			
		106	+ 4.2	
1163	25°53′			
		107	− 1.4	
1164	24° 6′			
		130	+10.5	
1165	22°35′			+3.6
		148	− 4.8	
1166	20°50′			
		155	+ 8.7	
1167	19°17′			
		145	+ 4.6	
1168	17°55′			
		135	− 0.1	
1169	16°22′			
		137	+ 0.4	
1170	14°47′			
		132	+ 7.7	+2.1
1171	13°15′			
		130	− 7.5	
1172	11°43′			
		122	+10.0	
1173	9°57′			
		88	+18.4	
1174	8°20′			
		102	−21.0	
1175	6°50′			
		138	− 2.4	
1176	5°16′			
		134	+ 6.9	
1177	3°13′			

The results of the dynamic calculations for the mid-Atlantic *Atlantis* section, however, give a small average velocity for this width, only 2.1 cm.sec.$^{-1}$ as shown in Table 4. For the adjoining band on the north side from 18°N. to 27°N. the average computed velocity is higher, namely 3.6 cm.sec.$^{-1}$ Hence it is necessary to revise the conclusion of the last paragraph and say that the North Equatorial Current extends in width at this surface and in mid-Atlantic from 10°N. to 27°N., and that the velocity distribution, except for station to station irregularities, appears fairly uniform.

Going back to Chart 9, this revised conclusion is not incompatible with the salinity distribution if it is remembered that considerable seasonal fluctuations are to be expected especially in the northern part of the area studied. According to yearly mean conditions at the sea surface, in conformance with which the chart was analyzed, salinities greater than 37.0 °/₀₀ along the $\sigma_t = 26$-line occur only where shown on the chart. Hence the

northernmost salt axis appeared necessarily to originate from there with the result that the intermediate fresher zone (which is somewhat poor in oxygen also) with salinities less that 36.9 °/₀₀ had to be an east current. In the different quarters of the year, however, salinities greater than 37.0 °/₀₀ and less than 36.75 °/₀₀ occur along the intersection with the sea surface in the part of the North Atlantic of present interest as follows:

Season	>37.0 °/₀₀	<36.75 °/₀₀
D-F	30°N.50°W. to 24°N.25°W.	east of 21°N.20°W.
M–M	30°N.50°W. to 22°N.22°W.	east of 22°N.21°W.
J–A	none	all
S–N	none	all except near 34°N.12°W.

The intersection with the sea surface is thus in general a source for salter water in winter and fresher water in summer. Therefore, the area indicated as a fresh (and O_2-poor) zone at about 19°N. is probably not a continuous zone, but rather the fresher water occurs in discreet areas which are of summertime origin at the sea surface, and which are moving west along with the salt water surrounding them.

The isentropic analysis of the salinity and oxygen distributions gives no evidence for the counter currents at 12½°N., 22°N. and 25°N. shown by the dynamic calculations. However, conclusive evidence against their existence is lacking.

The position of the principal fresh and O_2-poor axis in the North Equatorial Current was drawn to conform with the *Atlantis* mid-Atlantic section and the *Meteor* section of stations 296–305, which were made in March (1932) and April (1927) respectively. The *Dana* section of stations 1160–1174 was disregarded. This section, which was made in November (1921) crossed the minima of salinity and oxygen two degrees further south at about 8½°N. instead of 10½°N., between stations 1169 and 1171. Likewise the *Carnegie* stations made about the first of September (1928) indicate the fresh axis in the more southerly position; the average of four stations (23, 25, 26, 27) at 11°N. gives 36.04 °/₀₀, while station 24 at 8°N. gives 35.77 °/₀₀. The *Deutschland* section made in July (1911) runs nearly east-west in this region, but may be fitted into the analysis if the minimum of 35.61 °/₀₀ at station 23, 7°N., represents the position of the fresh axis when this section was made.

Evidence of a slight salinity maximum between 9°N. and 10°N. at the fortieth meridian is found at *Meteor* 302 and *Atlantis* 1173. This is ascribed to an eddy as indicated by the broken arrow. According to the dynamic calculations the highest west velocity anywhere along the *Atlantis* section coincides with this arrow. This cyclonic eddy, also found on the two deeper surfaces, has smaller dimensions on this surface and appears to be more intense. Again vertical motion within the eddy does not appear necessarily required.

The Equatorial Counter Current was not found on the two deeper surfaces except as the southern part of the cyclonic eddy, which however extended as a salt axis on the $\sigma_t = 26.5$-surface from 51°W. to about 37°W. On the $\sigma_t = 26$-surface, however, this same salt axis may be drawn so as to extend continuously across the entire Atlantic and may be identified definitely as the Counter Current. East of 45°W. it is also an O_2-rich axis. It is apparently supplied partly by water from the South Atlantic, especially at 45°W. and 35°W. as indicated by recurving arrows. In placing the axis where it crosses the *Atlantis* section, the results of the dynamic calculations have been disregarded; these give the maximum east velocity at 7½°N. instead of at 6°N.

The high salt content of the Counter Current offers an intriguing problem, for which

several possible solutions may be suggested. The difficulty is that the current starts in the west with a maximum salinity of about 36.9 °/₀₀ but it is cut off from the salt supply further north, only slightly salter than 36.9 °/₀₀, by the fresh axis of the North Equatorial Current with minimum salinity at least as low as 36.5 °/₀₀. This fresh axis appears to have a strong push so that its discharge into the Caribbean would be expected. It may be, however, that this discharge is only intermittent and that alternately salt water is supplied to the Counter Current either through the Caribbean or east of the Antilles. Another possibility is that the fresh axis does not discharge to the west, but recurves cyclonically before entering the Caribbean and returns eastward as part of the Counter Current, allowing an uninterrupted supply of salt water to the salt axis of the Counter Current. Or it may be that the motion is not isentropic and that the salt is derived from superior σ_t-surfaces. It will be found in the next chapter that the salinity distribution on the $\sigma_t = 25.5$-surface, which is similar to the one on this surface, is more easily explained, and that explanation probably applies to this surface also.

The supply to the North Equatorial Current of fresh water from the South Atlantic is indicated as entering along the African coast. This is a marked change from the analysis of the $\sigma_t = 26.5$-surface, where it was indicated as crossing the equator west of 30°W. The fresh water supplied along the African coast is already poor in oxygen, and consumption of oxygen along the fresh axis is not demanded.

South of the Counter Current is found the northern branch of the South Equatorial Current. It is shown by a fresh and O_2-poor axis extending, from somewhere east of 25°W., westward off the South American coast as far as the vicinity of Tobago and apparently entering the Caribbean.

A salter and O_2-rich tongue, which crosses the equator at 40°W., can be followed a short distance along the South American Coast. Most of the time it apparently mixes with the northern branch of the South Equatorial Current to form a current of intermediate salinity and O_2-content. Occasionally it appears to break through and supply oxygen to the Counter Current as indicated by the broken arrow. Perhaps, however, the increase within the Counter Current at 45°W. is due to the non-conservatism of O_2-content.

The analysis presented for this surface is admittedly only one possible interpretation of the data, but is the one which seems to the writer to give the most reasonable flow pattern. Another specific interpretation would be one consistent with the distribution of maximum salinity derived by Defant shown in Figure 3, which differs radically from that presented here.

IX. $\sigma_t = 25.5$-SURFACE (CHARTS 11–13)

31.65 (min.)	31.74	32.00	32.50	33.00	33.50	34.00	34.50	35.00	35.50	36.00	36.50	37.00	37.50 °/₀₀
−2.83°	0.00°	3.2°	6.8°	9.5°	11.7°	13.7°	15.5°	17.1°	18.7°	20.2°	21.5°	22.9°	24.2°

The greatest depth of this surface is 179 meters. Salinity ranges between 35.34 and 37.28 °/₀₀, temperature between 18.2° and 23.6°, oxygen between 2.20 and 5.25 cc.l.$^{-1}$ The extreme normal monthly displacements of the intersection of this surface with the sea surface occur in March and September, the positions in these two months being shown on Chart 11. The surface is closed to the Pacific Ocean in all quarters of the year, and is open to the Indian Ocean in D–F and M–M only.

The flow pattern derived for this surface is very nearly the same as for the $\sigma_t = 26$-surface. Again it must be said that while the pattern presented on the charts is the one which appears to the author to be at the same time in accord with the data as well as to give a reasonable interpretation, other interpretations of the plotted values are possible. Furthermore, some of the plotted values for this surface especially are uncertain due to interpolation between points widely spaced on the *t-S*-curves.

The average velocity of the North Equatorial Current, from the dynamic calculations for the *Atlantis* section, between 8°N. and 21°N. (stations 1166–1174) is 5.8 cm.sec.$^{-1}$ The average between 10°N. and 21°N. (stations 1166–1173), which gives a value more comparable with those stated for the deeper surfaces, is 3.6 cm.sec.$^{-1}$

As found in Chapter II, the tropospheric S-maximum occurs at a mean of $\sigma_t = 25.4$. Accordingly, of the surfaces studied, the S-maximum coincides most closely with the $\sigma_t = 25.5$-surface.

Parr's (1938b, Figure 12) chart of temperature on the $\sigma_t = 25.4$-surface serves qualitatively as a westward extension of Chart 12. According to it there is no temperature maximum west of the Lesser Antilles associated with the high temperature at *Atlantis* 2746 which appears to form the upstream end of the Equatorial Counter Current on Chart 12. This indicates no flow either into or out of the Caribbean at this point, although north of it water warmer than 23.4° (>39.19 °/$_{oo}$) enters the Caribbean all the way between Montserrat and Martinique.

Since this surface (either $\sigma_t = 25.4$ or $\sigma_t = 25.5$) is so near the vertical S-maximum, it is impossible that the high salinities at *Atlantis* 2746, *Dana* 1182 and stations further southeast can be the result of vertical mixing. They are, furthermore, cut off from the South Atlantic by much lower salinities, as was the case on the $\sigma_t = 26$-surface. Hence this water must have originated (at least approximately) at the intersection of the $\sigma_t = 25.5$-surface with the sea surface in the North Atlantic, have flowed west-southwest in the North Equatorial Current, and have recurved southeastward only slightly east of the Lesser Antilles. This being the case, it can hardly be doubted that the Counter Current has its source in this region of recurving.

It does not seem possible to say whether the supply of salt water is essentially continuous or whether it is intermittently interrupted by the westward discharge of the fresh tongue of the North Equatorial Current. A comparison of the three available charts of the distribution of S-maxima, namely Parr's for January 1937 (1938b, Figure 13) and for 1933 and 1934 combined (1937, Fig. 41) and Defant's (1936, Beilage XLIV) composite chart, indicates that conditions are indeed unsteady. But the low S-maxima appearing on the last two charts west of the Lesser Antilles at 15°N. may be the result of vertical mixing produced at the islands, rather than to the actual penetration of the fresh tongue into the Caribbean.

The analysis for this surface may be compared with Defant's analysis of the S-maximum, which resulted in the circulation scheme of Figure 3. Defant first points out the Southern Hemisphere Undercurrent along the South American coast, shown by a tongue of high salinity crossing the equator at 40°W. and traveling northwest through *Atlantis* 1178, *Meteor* 297, 294, 290 and *Carnegie* 29. According to my analysis this tongue extends only a few degrees north where it disappears due apparently to strong lateral mixing with the northern branch of the South Equatorial Current, which thereby becomes salter, whereas *Meteor* stations 294 and 290 lie in the Counter Current and their water of high salinity has come from the North Atlantic. The discrepancy may be re-

solved to the question whether the high salinity of 36.73 °/₀₀ on the $\sigma_t = 25.5$-surface at the isolated station *Meteor* 294, 7°N. 48°W., comes from the southeast or from the northwest. It is separated from 36.69 °/₀₀ 480 miles southeast by the *Meteor* section with maximum station value of only 36.30 °/₀₀ at station 297, which was made only 17 days later than station 294. On the other side it is separated from 36.68 °/₀₀ 380 miles northwest and 36.76 °/₀₀ 640 miles northwest (and even higher values at *Atlantis* 1201 and 1202 as well as at stations further northwest) by another *Meteor* section with maximum station value of 36.51 °/₀₀ at station 290 made only 4 days prior to station 294 (or 36.66 °/₀₀ at station 292). The latter route, which is the route of the Counter Current according to my analysis, appears to be in better accord with the data.

Defant indicates the Undercurrent as continuing from *Meteor* 290 north of *Carnegie* 30 at 13°N. 56°W. If his analysis is correct, it follows that the fresh tongue of the North Equatorial Current, the Counter Current and the northern branch of the South Equatorial Current are all limited in their westward extension by this Undercurrent. He places the origin of the Counter Current at 10°N. 40°W. Hence there is a very real discrepancy with my analysis.

It is even questionable as to whether the high salinity near the equator and 40°W. is of South Atlantic origin. I have constructed the necessary t-S-diagrams and find, on proceeding southward across the *Meteor* sections south of the equator, the following S-maxima at the $\sigma_t = 25.5$-surface:

Station, *Meteor*	256	207	252	204
Latitude, S.	2°3′	5°48′	6°51′	12°45
Salinity, °/₀₀	36.51	36.63	36.50	36.70

Hence the high values in question are cut off from the south also, but to less degree than from the northwest. It still appears as a possibility, however, that they have originated from the northwest past *Meteor* 292. Such a flow would constitute a salt counter current south of the northern branch of the South Equatorial Current.

Defant's analysis agrees in showing the broad flow of fairly uniform direction from the northeast quadrant toward the Antilles (which he calls Northern Hemisphere Undercurrent, but which is here called the salt half of the North Equatorial Current), part of which he says enters the Caribbean and part flows north of Haiti. His current arrows have a slightly greater component equatorward than mine.

As mentioned above, the source region for his Counter Current is 8°N. to 12°N. and 36°W. to 44°W., whereas according to my interpretation the current can be traced from 60°W. and is further south in mid-Atlantic. He says it is fed from the North Equatorial Current and from the salt Southern Hemisphere Undercurrent. He demonstrates the northern branch of the South Equatorial Current as a fresh tongue, which however stops at 40°W. Defant does not consider the fresh zone north of the Counter Current to be part of the North Equatorial Current, but to be a line of convergence from which water is removed above, so that the vertical S-maximum is destroyed, in accordance with its observed absence at most stations within the zone as far west as 44°W. He indicates an east flow in this zone, evidently because progressive vertical mixing with deeper water on moving downstream would give progressively lower S-values as observed. Furthermore he indicates no west flow between the Counter Current and Cape Palmas, which would supply fresh water to this zone.

Hence the method used here, which is based on the permissibility of lateral mixing only for altering salinity along trajectories, leads to the opposite sense of flow within this

fresh zone from that derived by Defant's method, which is based on the permissibility of vertical mixing and non-isentropic flow. There are two general attacks suitable for trying to determine which of these methods or results is more nearly correct. The first is based on the observed distribution of sea water properties and on available knowledge of mixing coefficients. West of 23°W. the zone in question is deeper than 50 meters according to Chart 11. According to Figure 5, furthermore, surface densities over nearly the whole zone are less than $\sigma_t = 24.25$. Accordingly it seems impossible that vertical mixing and surface effects can extend downward even beyond the $\sigma_t = 25.5$-surface as demanded by Defant's analysis, although no numerical evidence in support of this statement is presented. While Defant's whole treatment of this zone appears to be an attempt to explain the absence of a vertical S-maximum, it may more simply be regarded as a coincidence that the low salinity tongue supplied from the South Atlantic has approximately the same salinity as the superior σ_t-surfaces and as the sea surface.

The other attack would be to try to determine the sense of the flow along the zone in question by independent means. The fresh axis crosses the mid-Atlantic *Atlantis* section between stations 1173 and 1174 where the dynamic calculations give the highest velocity of the North Equatorial Current (22 cm.sec.$^{-1}$ at the $\sigma_t = 25.5$-surface). The density distribution on the *Carnegie* section, on the other hand, indicates an east gradient current between station 24 and the pair 23 and 25. On the *Meteor* section crossing the zone obliquely at about 38°W. a west gradient current is indicated between stations 301 and 303 (Wüst und Defant, 1936, Beilage CII). Further east, unfortunately, no sections cross the zone. This evidence is meagre and conflicting, but favors slightly the results obtained by the isentropic analysis.

The analysis here presented rests on the assumption that there is a strong supply of fresh water from the south along the African coast. It would be advantageous to determine the correctness of this assumption.

Providing it is true that the fresh tongue is part of the North Equatorial Current and flows west, a definite conclusion regarding the relative importance of vertical and lateral mixing is possible. Since this surface is near the vertical salinity maximum, vertical mixing alone would produce lower salinities downstream. Actually higher salinities are found downstream, so lateral mixing with the salter water on each side is more effective in changing the salinity of the tongue than is vertical mixing. Table 5 illustrates the increase in salinity along this tongue. The average at the S-maximum along this tongue is actually $\sigma_t = 25$, but since the same fresh tongue apparently moves west on the $\sigma_t = 25$-surface also (see Chart 15), and since the S-maxima increase downstream also, the conclusion is not affected.

TABLE 5

STATION VALUES OF SALINITY ON PASSING WESTWARD ALONG THE FRESH AXIS OF THE NORTH EQUATORIAL CURRENT

STATION	LONGITUDE	$\sigma_t = 25.5$-SURFACE	S-MAXIMUM	
		S	S	σ_t
Meteor 267	19°49′W.	35.57 °/₀₀	35.61 °/₀₀	25.8
Meteor 303	37°31′	35.85	none	
Atlantis 1174	40°45′	35.84	35.84	25.5
Deutschland 21	43°54′	35.85	35.91	24.7
Dana 1171	44°35′	36.16	36.33	24.4
Meteor 289	49°33′	36.38	36.41	25.7
Carnegie 30	56°15′	36.46	36.56	25.0
Dana 1181	57°20′	36.40	36.68	24.8
Challenger 1328	59°24′	36.62	36.70	25.1
Atlantis 2745	60°28′	36.59	37.00	24.9

For each of the deeper surfaces a small table of salinity ranges at the intersections with the sea surface was presented. It is omitted for this surface because conditions are similar in both oceans and Chart 12 itself gives the more important values for the North Atlantic. In the present case the most interesting fact to be obtained from Figure 5 is that the $\sigma_t = 25.5$-line passes through the North Atlantic maximum of salinity at the sea surface, >37.25 °/₀₀ at 25°N. 40°W. This is found to agree with the σ_t-value at which the vertical S-maximum is found for stations which lie, according to Defant (1936, Beilage XLIV), near the origin of the S-maximum layer in the North Atlantic, namely a mean of $\sigma_t = 25.6$, and with the highest S-maximum of 37.20 °/₀₀, as shown on the left of Table 6. In this table the salinities are from Defant's (1936, p. 372 ff.) table, the σ_t-values from t-S-curves (see p. 16). It will be noticed that, while the S-maxima at all stations as given in Table 1 are rather scattered, the stations close to the sources have maxima closely grouped about the mean values, and there is a distinct difference between the North and South Atlantic. The mean of $\sigma_t = 24.9$ with highest salinity 37.22 °/₀₀ for the South Atlantic again agrees with the position of the $\sigma_t = 25$-line at the sea surface, which passes through the highest salinity in the South Atlantic, >37.25 °/₀₀ at 16°S. 30°W.

TABLE 6

σ_t AND SALINITY AT S-MAXIMUM FOR STATIONS NEAR THE SOURCE OF THE S-MAXIMUM LAYER

North Atlantic			South Atlantic		
Station	σ_t	S	Station	σ_t	S
Atlantis 1168	25.3	37.13			
1169	25.2	37.08			
Challenger 1326	25.1	37.20	*Meteor* 158	24.8	37.22
Deutschland (Reihe) 19	25.7	37.02	202	25.0	37.05
Meteor 281	25.8	37.10	203	25.0	37.08
282	25.7	37.10	204	25.0	37.16
283	25.6	37.05	205	25.0	37.16
284	25.9	37.05	207	24.9	37.15
285	25.7	36.97	252	24.9	37.01
286	25.8	37.01			
Mean	25.6			24.9	

Herein lies the simple explanation of the occurrence of the S-maximum layers in the two oceans, and of the potential densities at which they occur. Defant's statement, that the S-maximum layer has its origin in the deepest part of the subtropical reservoirs of water of high salinity (see p. 9), gives a somewhat false impression.[8] Actually the homogeneous surface layer of the subtropics is convergent over a large area and this convergence is compensated by a slow flow downward with an equatorward component along surfaces of constant potential density. The particular potential density surface which comes to the sea surface at the highest surface salinity becomes the S-maximum surface.

[8] The writer feels sure, furthermore, that the S-maximum layers which Defant (1936, Beilage XLIV) finds on the poleward sides of the subtropical regions without S-maxima can also be explained on the basis of isentropic flow, but this lies outside the scope of the present paper.

X. $\sigma_t = 25$-SURFACE (CHARTS 14–16)

31.04 (min.)	31.11	31.50	32.00	32.50	33.00	33.50	34.00	34.50	35.00	35.50	36.00	36.50	37.00	37.50 °/oo
−2.70°	0.00°	4.3°	7.6°	10.1°	12.3°	14.2°	16.0°	17.6°	19.2°	20.6°	22.0°	23.3°	24.6°	25.8°

The greatest depth of this surface is 145 meters. Salinity ranges between 35.06 and 37.17 °/oo, temperature between 19.30° and 25.00°, oxygen between 2.35 and 5.70 cc.l.$^{-1}$ The surface is closed to the Pacific and Indian Oceans in all quarters of the year, so the waters on it are of purely Atlantic origin.

The following small table gives the range of salinity at the intersection of this surface with the sea surface in the South Atlantic. The isolated $\sigma_t = 25$-surface surrounded by higher surface densities which appears on several of Böhnecke's charts (yearly mean, J–A, S–N) along the coast of South America in the vicinity of the Plata River is omitted from consideration. The minimum salinity at the African coast is given in the last column.

Year			
D–F	10°–26°S.	35.5–37.3 °/oo	35.5 °/oo
M–M	10°–42°	33.7–37.6	35.2
J–A	14°–42°	33.3–37.3	35.7
S–N	8°–17°	35.5–37.3	35.5
	8°–16°	35.7–37.2	35.7

This table is presented primarily for the discussion of the fresh water found along the African coast on Chart 15. This is probably cut off entirely from the very low salinities found near the Plata River in the quarters D–F and M–M, and originates in the tropical eastern Atlantic. At the intersection of the $\sigma_t = 25$-surface with the sea surface at the African coast in the South Atlantic, however, the lowest salinity according to the table is 35.2 °/oo. Since a lower value, 35.06 °/oo, is found at *Meteor* 219 as shown on Chart 15, and since there must be a strong supply of fresh water if the analysis presented is correct, it appears probable that this supply has been freshened to at least some extent by vertical mixing with the very fresh superior water in the Gulf of Guinea or at Cape Palmas.

The dynamic calculations for the mid-Atlantic *Atlantis* section give the following values for the west component of the gradient current on this surface:

Latitude, N.	3°13′	5°16′	6°50′	8°20′	9°57′	11°43′	13°15′	14°47′	16°22′
Station	1177	1176	1175	1174	1173	1172	1171	1170	1169
Depth, meters	108	110	74	63	98	110	100	78	
Velocity, cm.sec.$^{-1}$	+17.5	−11.6	−37.0	+24.1	+18.9	−10.0	+9.6	−2.6	

The average for the North Equatorial Current between 8°N. and 16°N. is 8 cm.sec.$^{-1}$ The east current between stations 1169 and 1170 corresponds to Iselin's counter current mentioned in Chapter V.

The circulation found for this surface is much the same as for the $\sigma_t = 25.5$-surface, so it requires no further individual discussion. The following special problem is however fittingly inserted in this chapter.

Isentropic analysis in itself does not yield more than the direction of velocity; its magnitude can be determined only by use of supplementary information. The possibility was suggested at the end of Chapter III that the convergence of the drift current might be used quantitatively to determine horizontal velocities. The analyses of the $\sigma_t = 25.5$-surface and of the $\sigma_t = 25$-surface offer an example convenient for the trial of this hypothesis.

The tube is selected which is bounded by these two surfaces and by the verticals at *Atlantis* stations 1169 and 1171. From Chart 12 it is seen that the streamline through

station 1169 may be identified with the salt axis, and that through 1171 with the $S = 36.5$-line. The basis for the latter is that it lies about midway between the fresh and salt axes, where salinity would be fairly constant along a streamline. Similarly from Chart 15 the streamline through station 1169 may be identified with the $S = 37.0$-line, and that through 1171 with the $S = 36.5$-line. These four streamlines bounding the tube of roughly rectangular form are shown in Figure 9. It is seen that the horizontal projections of the upper and lower surfaces of the tube coincide rather closely. The open mouth

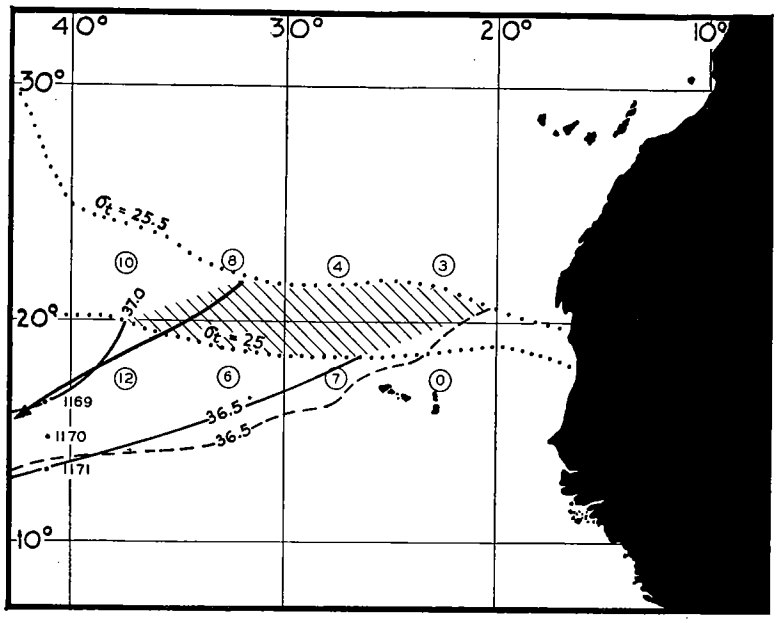

FIG. 9.—Streamline tube. Dotted lines are density lines at sea surface. Arrow is salt axis and broken line is isohaline on $\sigma_t = 25.5$-surface. Full lines are isohalines on $\sigma_t = 25$-surface. Open mouth of tube shown by hatched area. Numbers in circles are convergence of drift current in cm. per day.

of the tube, or its intersection with the sea surface, covers 41 one-degree squares or about $40 \cdot 10^{14}$ cm.^{2} The depths in meters of the upper and lower boundaries along the *Atlantis* section are as follows:

STATION	$\sigma_t = 25$	$\sigma_t = 25.5$	DIFFERENCE
1169	60	100	40
1170	96	123	27
1171	104	110	6

The average height of the tube at the section is thus 25 meters and its width 3°7′ (312 km.), so its area here is approximately $8 \cdot 10^{10}$ cm.^{2} The ratio of the area at the mouth to that at the *Atlantis* section is $5 \cdot 10^4$. The average convergence of the drift current (for mean July[9] conditions, from Montgomery 1936, Fig. 1) over the mouth of the tube is about 6 cm. per day or $7 \cdot 10^{-5}$ cm.sec.$^{-1}$ Multiplying this by the ratio of areas gives the average west velocity in the tube at the *Atlantis* section, 3.5 cm.sec.$^{-1}$

The reasonableness of the resulting velocity lends weight to the method used, and

[9] According to Mr. Brooks' computation for January (see footnote 7) the average convergence is 16 cm. per day or $18.5 \cdot 10^{-5}$ cm.sec.$^{-1}$, giving a velocity at the *Atlantis* section of 9 cm.sec.$^{-1}$

gives some supporting evidence to the assumptions involved. It may be compared with the velocities from the dynamic calculations for the two halves of the tube: average of 1.6 cm.sec.$^{-1}$ east for the tube between stations 1169 and 1170, average of 9.1 cm.sec.$^{-1}$ west for the tube between stations 1170 and 1171.

XI. $\sigma_t = 24$-SURFACE (CHARTS 17–19)

29.82 (min.)	29.88	30.00	30.50	31.00	31.50	32.00	32.50	33.00	33.50	34.00	34.50	35.00	35.50	36.00	36.50	37.00 °/₀₀
−2.43°	0.00°	2.0°	6.2°	9.1°	11.4°	13.5°	15.3°	17.0°	18.6°	20.1°	21.5°	22.8°	24.1°	25.4°	26.6°	27.8°

The greatest depth on this surface is 122 meters. Salinity ranges between 34.88 and 36.71 °/₀₀, temperature between 22.50° and 27.10°, oxygen between 3.33 and 5.40 cc.l.$^{-1}$

The following small table gives the range of salinity at the intersection of this surface with the sea surface in the South Atlantic. In each case the lowest salinity occurs at or near the coast in the Gulf of Guinea. Each of Böhnecke's charts shows an isolated $\sigma_t = 24$-surface at the mouth of the Plata River; the low salinities there are omitted from the table.

Year		
D–F	0°–12°S.	35.5–36.5 °/₀₀
M–M	0°–14°	35.2–36.5
J–A	6°–13°	35.0–37.0
S–N	0°– 9°	34.5–36.3
	0°–10°	35.4–36.3

It again appears probable that the low salinities (34.88 and 35.10 °/₀₀) found near the African coast at 10°N. have been accentuated by vertical mixing with the superior fresher water, either locally or in the Gulf of Guinea.

There is not much contrast between the density of this surface and density at the sea surface; surface density above a small percentage only of the area of the $\sigma_t = 24$-surface is less than $\sigma_t = 23$. According to yearly mean conditions it appears that this surface has several internal boundaries or holes as indicated on Chart 17. Only about half of its area at any one time is permanently present in all seasons. Its depth is found to be 100 meters or more at only four stations. From these statements it might be expected that surface influences and vertical mixing would be so effective, and that seasonal and irregular fluctuations would make the non-synoptic observations so inconsistent, that an isentropic analysis for this σ_t-surface would not be a fruitful undertaking. It is nevertheless found that an analysis of this surface may be carried out in the same way as for the deeper surfaces. This lends some support to the hypothesis that even on this surface the motion is largely isentropic.

As on the deeper surfaces the fresh and O_2-poor axis of the North Equatorial Current occurs at about 10°N., but the surface is so limited on the north side that the salt axis does not appear. Immediately south of this fresh axis is found the salt and O_2-rich axis of the Equatorial Counter Current, which is especially marked in the salinity distribution where it is shown by S-maxima at all five sections which it crosses. Still further south there is a fresh and O_2-poor west current, the northern branch of the South Equatorial Current, indicated by S-minima at all five sections it crosses. The salt axis along the South American coast is again present, the sense of the motion being apparently northwest.

While on the $\sigma_t = 25$-surface the Counter Current and the northern branch of the South Equatorial Current were placed at 6°N. and $4\frac{1}{2}$°N. respectively in mid-Atlantic,

on this surface they are placed at 8°N. and 6°N. These positions appear to be in best accord with the salinity distributions on the two surfaces. It is unlikely, however, that an eastward axis on the lower surface and a westward axis on the higher surface should both occur at 6°N. Furthermore, both the navigational record and the dynamic calculations for the *Atlantis* sections give an east current at this latitude. It is therefore quite likely that the northern branch of the South Equatorial Current has been placed too far north on the charts for the higher surface.

The origin of the salt water supplying the upstream end of the Counter Current was discussed in Chapters VIII and IX, with the conclusion that it must flow in from the north along the east side of the Lesser Antilles. On the $\sigma_t = 24$-surface, however, the path of this salt tongue shows up directly in the salinity distribution. While the interpolations on the t-S-diagrams for the stations delineating this tongue are quite reliable, the stations are relatively few and non-synoptic, so it is possible that the continuous tongue on Chart 18 is fictitious.

If this salt tongue is a permanent feature, it follows that the fresh tongue of the North Equatorial Current is completely absorbed by the Counter Current, which would account for the rapid decrease in salinity of the latter between 55°W. and 40°W. Such a permanent fresh tongue, furthermore, limits the types of water which can enter the Caribbean on this surface to (1) North Atlantic water sinking along the intersection with the sea surface west of about 50°W. (the convergence of surface water is strong west of this longitude) and to (2) possibly small amounts of fresher water entering past Trinidad. That the salinity lines on Chart 18 do not show the former may be ascribed to their being drawn in accordance with non-synoptic station values as well as with mean sea surface salinities.

This discovery, that the motion east of the Lesser Antilles has no strong west component as has been generally supposed, finds a parallel in the distribution of salinity at the sea surface. In the months from May to August low salinity water originating from the Amazon discharge moves north-northwest as far as 20°N. (Böhnecke, 1936, Beilage XXXVI–XXXIX). Thus there is no strong west component at the sea surface either. Since the water moves nearly normal to the easterly winds in this region, it is evidently transported chiefly by the drift current, only to small extent by any other type of flow. Just below the surface layer, which alone is directly affected by the wind, the return southerly flow occurs as indicated on the $\sigma_t = 24$-surface.

Not only have the isohalines been drawn so as to end along the intersections with the sea surface at the points demanded by mean surface conditions, but also the arrows have been drawn to agree with the probable positions of sources and sinks at these intersections. A strong sink is indicated at the African coast at 14°N., corresponding to the divergence of surface water there. Between 20°W. and 40°W. the fresh tongue of the North Equatorial Current parallels the intersection with the sea surface, indicating neither source nor sink; this agrees with the probable position, about 12°N., of the boundary between the subtropical convergence of surface water and the equatorial divergence of surface water. Further west the intersection is undoubtedly a source. Arrows have been drawn to indicate that the two internal boundaries at 0°N. 24°W. and 4°N. 45°W., lying in the equatorial zone, are sinks.

The salinity distribution at this surface is remarkably different from that at the sea surface (see Fig. 5). The latter is simpler. Between 20°W. and 40°W. a fresh zone is centered at 7°N. to 8°N. with lowest values 34.7 to 35.5 °/₀₀; northward and southward

from this zone salinity increases fairly uniformly. Thus there is no indication at the sea surface of the salt Counter Current.

Even for this σ_t-surface, which is so near the sea surface, it appears that surface influences and vertical mixing may be considered of secondary importance except along the African coast, and the advantage of isentropic analysis is demonstrated.

The flow pattern derived may be compared with that computed by Defant in his study of the layer of maximum vertical density gradient (see p. 6). The latter also indicates the presence of the North Equatorial Current, the Counter Current, and the northern branch of the South Equatorial Current, but gives the Counter Current greater breadth so that it occupies the zone from 4°N. to 10°N. approximately. He indicates a northwest flow all along the South American coast, even in the region occupied by the Counter Current west of 50°W. according to Chart 18. Along the African coast his flow is *into* the Gulf of Guinea.

XII. SUMMARY OF THE CIRCULATION OF THE UPPER SUB-SURFACE LAYERS OF THE SOUTHERN NORTH ATLANTIC

The predominant current of the region investigated is the North Equatorial Current, running west. It appears to originate quite close to the African coast, only about 200 miles offshore, and flows west with a small south component over most of its course, as far as about 60°W., there partly recurving cyclonically, partly discharging into the Caribbean and partly continuing north of the West Indies as the Antilles Current. Its southern boundary occurs in mid-Atlantic at about 9°N. Its northern boundary occurs at roughly 30°N., but further north in the east and further south in the west, and its position is probably seasonally variable. The northern half is characterized by high salinity and high O_2-content, while near the southern edge the current contains an axis of low salinity, which is O_2-poor.

This regime holds in general on all six surfaces analyzed, but on the deepest surface ($\sigma_t = 27$) the southern part of the Equatorial Current recurves at about 45°W. to form a large cyclonic eddy of about 750 miles diameter. This occurs to somewhat less degree on the next higher surface ($\sigma_t = 26.5$) also. The northern part of the current of course does not appear on the highest surfaces as these are of too limited extent.

It appears probable that velocity is fairly constant across the North Equatorial Current in mid-Atlantic, except that quite likely the greatest velocity occurs close to the southern edge. Average velocities from dynamic calculations increase from 1.7 cm.sec.$^{-1}$ for the $\sigma_t = 27$-surface to 5.8 for the $\sigma_t = 25.5$-surface and 8.0 for the $\sigma_t = 25$-surface. For the depth of these surfaces in mid-Atlantic see Figure 7. No conclusion seems possible as to whether the current has a fine structure, i.e. whether it contains counter currents or eddies (of diameter up to 200 miles) as indicated by the dynamic calculations.

Sections crossing the fresh axis of the North Equatorial Current in March and April indicate it as lying about 150 miles further north than do the sections made in July, September and November, especially on the $\sigma_t = 26$-surface.

At the origin of the North Equatorial Current in the eastern Atlantic, it is supplied with salt, O_2-rich water from the North Atlantic. At the $\sigma_t = 27$-surface this supply of water may have received some of its salt from the Mediterranean outflow, but at the

$\sigma_t = 26.5$-surface and higher surfaces the water has originated entirely at the sea surface in the North Atlantic. At its origin the current is supplied also with fresh, O_2-poor water from the South Atlantic. On the two deeper surfaces ($\sigma_t = 27$, $\sigma_t = 26.5$) this supply appears to cross the equator at about 30°W. as an O_2-rich axis, but its O_2-content there is decreased by about 50% before it reaches the origin of the Equatorial Current. On the higher surfaces the fresh supply comes in along the African coast, and no noticeable decrease in O_2-content takes place. On the two highest surfaces ($\sigma_t = 25$, $\sigma_t = 24$) the fresh supply originates at the sea surface in the tropical eastern South Atlantic, but it appears to have been further freshened by vertical mixing with the very fresh superior water along the equatorial coast of Africa.

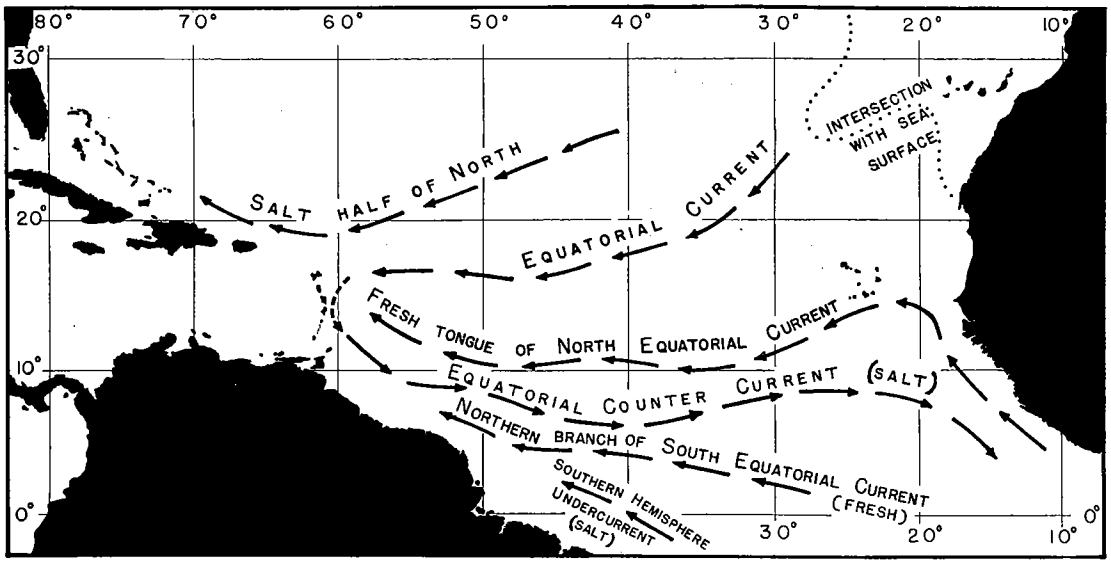

FIG. 10.—Outstanding features of the flow pattern on the $\sigma_t = 26$-surface.

The Equatorial Counter Current appears on the four higher surfaces ($\sigma_t = 26$, 25.5, 25, 24), at 6°N. or 8°N. in mid-Atlantic, as a band 100–150 miles broad flowing east toward the Gulf of Guinea and originating, as shown for the first time, nearly at the Antilles. It is characterized by relatively high salinity and high O_2-content. While during its course lateral mixing occurs with the fresher water of South Atlantic origin both north (North Equatorial Current) and south (northern branch of the South Equatorial Current) of it, at its source it is composed essentially of salt North Atlantic water.

The high salt content of the Counter Current is of considerable significance, as it must be supplied by a southward flow immediately east of the Lesser Antilles (possibly west of these islands). If this is an intermittent flow, the fresh tongue of the North Equatorial Current can discharge into the Caribbean only intermittently. If it is a permanent flow, the fresh tongue must be completely absorbed by the Counter Current, and no South Atlantic water enters the Caribbean at these surfaces except perhaps along the coast of South America.

The northern branch of the South Equatorial Current also appears on the four higher surfaces, as a fresh, O_2-poor tongue immediately south of the Counter Current.

Evidently crossing the equator somewhere east of 20°W., it extends as far west at least as 50°W. On the $\sigma_t = 26$-surface it apparently enters the Caribbean in the vicinity of Tobago, but on the higher surfaces its identity west of 50°W. is not clear. On these higher surfaces its water may reach to the Caribbean also, or it may be absorbed by the Counter Current.

Conditions are rather complicated and uncertain along the South American coast between 40°W. and 60°W. On the two deeper surfaces ($\sigma_t = 27$, 26.5) a fresh and O_2-rich current from the South Atlantic with its axis about 175 miles offshore flows northwest and apparently enters the Caribbean.

On the four higher surfaces ($\sigma_t = 26$, 25.5, 25, 24) this single current appears to be replaced by the Equatorial Counter Current, the northern branch of the South Equatorial Current and the Southern Hemisphere Undercurrent. The latter is a salt and O_2-rich tongue (the Atlantic origin of which was questioned in Chapter IX, but) which supposedly has its source in the area of high salinity at the sea surface in the South Atlantic, and is most pronounced on the $\sigma_t = 25$-surface. It crosses the equator at 40°W. flowing west-northwest and can be traced only as far as 46°W. or 48°W. It is apparently absorbed by the northern branch of the South Equatorial Current, and from the highest surface ($\sigma_t = 24$) a large part of it is lost to the surface layer. While the Southern Hemisphere Undercurrent seems to be in immediate contact with the coast on the $\sigma_t = 26$-surface, on the higher surfaces, due to the gradual slope of the continental shelf, it is somewhat separated. Between it and the coast on these higher surfaces there may be a fresh current somewhat poor in oxygen which parallels it and which may well extend as far as Trinidad (West Indies), as indicated on the charts for the $\sigma_t = 25.5$-surface.

The outstanding features of the flow patterns on the four higher surfaces being similar, it is possible to represent these by a single schematic chart as in Figure 10. This is based on the deepest of these four higher surfaces, the $\sigma_t = 26$-surface, but the successively higher surfaces differ chiefly only in that the intersection with the sea surface retreats toward lower latitudes.

XIII. CONCLUDING REMARKS

The descriptive results summarized in the preceding chapter, which differ in important respects from any obtained previously, were derived chiefly from the distributions of salinity and O_2-content on surfaces of constant potential density, or rather, which for practical purposes is equivalent (see Chapter III), on σ_t-surfaces. Such a distribution, it should be emphasized, differs markedly from the distribution of salinity or O_2-content on level surfaces, as may be seen easily by comparing the present charts with any charts for fixed levels in the same region (for instance with the salinity distribution at 200, 400 and 600 meters in the Atlantic Ocean by Wüst and Defant, 1936, Beilage LXII–LXIV).

The reasons for representing the distributions of observed properties in this manner were outlined in the Introductory Statement and extended in Chapter III. As these concepts have not been explicitly and fully stated before, it is appropriate to list here that evidence, both unfavorable and favorable, which may be gleaned from the preceding chapters concerning their general validity.

Non-isentropic mixing of far-reaching effect takes place at the Straits of Gibralter. Vertical mixing is found along the African coast also between the Gulf of Guinea and

about 15°N., apparently at least as deep as the $\sigma_t = 25$-surface. The possibility of very intense vertical mixing at *Atlantis* 1200 and 1201 near the South American coast was mentioned in Chapter VI. All these occur along coastlines, however, and the bottom friction in shallow water is probably essential for bringing about such cases of non-isentropic mixing. Conclusive evidence against the concepts in question would be the discovery of a region on the σ_t-surface characterized by permanently closed isohalines, or a permanently closed, O_2-rich region below the greatest depth of photosynthesis. It is notable that the charts show no evidence of such regions.

The findings at the end of Chapter IX show definitely that the flow of the S-maximum layer is isentropic and that its source is at the intersection of its potential density surface with the sea surface, or, more precisely, with the vertically homogeneous surface layer. Since the agreement in salinity and σ_t was found to be so close between the S-maximum layer and maximum salinity at the sea surface, it must be concluded that the schematic representation in Figure 4 is closely fulfilled, namely that surface influences and vertical mixing are limited to the homogeneous layer. The result of the example of a stream line tube treated numerically in Chapter X also supports these conclusions.

In Chapter IX it was pointed out that at about $\sigma_t = 25$ there is a zone at about 10°N. which is a S-maximum vertically and a S-minimum laterally, and that its salinity increases westward. Unfortunately the sense of the motion (if any) of this zone is not known definitely, but probably the zone is part of the North Equatorial Current. In that case the preponderance of lateral over vertical mixing, as far as this zone is concerned, is clearly demonstrated.

The conditions on the $\sigma_t = 24$-surface, while density at the sea surface above most of its area is greater than $\sigma_t = 23$, give a picture markedly different from the salinity distribution at the sea surface. This indicates that, even at this high level, the flow is largely isentropic and that surface influences and vertical mixing must be limited to approximately the homogeneous surface layer.

Finally, a self-contained, consistent flow pattern for each of the six surfaces was obtained on the basis of the concepts in question. All this evidence together, while not conclusive, makes it appear probable that these concepts are generally valid to a rather close approximation.

Aside from the primary purpose of this investigation, two items of general significance have received particular attention. One was to demonstrate, in Chapter V, the validity and practical procedure of a method of dynamic calculations, using a function named "geostrophic potential," suitable for the representation of gradient flow on a σ_t-surface.

The other was the computation of transport through a streamline tube from the convergence of the drift current at its mouth (Chapter X). The reasonableness of the resulting mean horizontal velocity gives some justification to the assumptions involved, including the assumption that the convergence of the drift current represents the total convergence of the homogeneous surface layer. If this is generally true, it appears that the method has further applicability as a means of determining the magnitude of velocities within the troposphere.

An obvious paradox is reached, however, if motion below the surface layer is completely isentropic, and if at the same time the convergence, both positive and negative, of the drift current represents the total convergence of the surface layer. The latter would demand, in order that continuity be maintained, that the equatorial regions of strong divergence of the drift current be supplied with water from the subtropics by a

path lying below the surface layer. According to the former, such a compensating flow is impossible because surface density is markedly less in equatorial than in subtropical regions. The simplest modification which might bring these two concepts into agreement with actual conditions would be to drop the hypothesis that the *sinks* for a surface of constant potential density must always occur at its intersection with the sea surface. While direct evidence was found that at least some of the sources lie at the sea surface intersection, in no case was it found that the sinks do also. Thus upwelling from moderate depths could be permitted in equatorial regions.

This upwelling need occur only as follows: If there is horizontal divergence of surface water in a region, like the equatorial region, where the isopycnal surfaces near the sea surface are essentially horizontal, the divergence cannot be compensated by isentropic inflow from below. As a consequence the lower boundary of the homogeneous surface layer is restrained to an elevated position near the sea surface. Vertical turbulence continually mixes the water immediately below the boundary with the surface layer, thus accomplishing the compensating inflow of water from below by means of "mixing upward." This vertical mixing, however, would certainly not be expected to extend deeper than the theoretical depth of frictional influence, which depends on wind speed and latitude, for steady conditions in a homogeneous ocean (Rossby and Montgomery, 1935, p. 64 ff.).

The author fully realizes that the present paper is purely qualitative in character. Quantitative treatment of many phases is sorely needed, especially determination of lateral mixing coefficients, as Grimminger (1938) has done for isentropic charts of the atmosphere, and their application, together with a suitably chosen velocity distribution, to the task of testing whether the flow patterns which have been derived conform to continuity of mass and salt.

On the basis of the concepts presented it is possible to outline a few hypotheses which might serve as a suitable simplified groundwork for any study of the circulation of the oceanic trophosphere. These will be stated briefly, without qualifying restrictions, in three parts.

(1) The drift current and surface temperature, and to less extent surface salinity, are controlled by a balance with atmospheric conditions and with radiation through the atmosphere. Hence these three items may be regarded as climatic conditions which are externally prescribed and represent the fixed boundary conditions for the ocean below the surface layer.

(2) The total horizontal convergence or divergence of the surface layer is given by the convergence or divergence of the drift current. If annual and other fluctuations are left out of account, convergence (positive only) is exactly compensated by downward isentropic flow. Divergence may be compensated by "mixing upward" from layers of somewhat greater density.

(3) Except in the case of the upwelling just mentioned, vertical diffusion and viscosity may be neglected below the surface layer. Due to the action of bottom friction in producing non-isentropic mixing, they are, however, of importance along coastlines.

REFERENCES

BJERKNES, V. F. K., und verschiedenen Mitarbeitern
1912. Hydrographische Tabellen. Dynamische Meteorologie und Hydrographie, Druck und Verlag von Friedr. Vieweg & Sohn.

BÖHNECKE, GÜNTHER
1936. Atlas zu: Temperatur, Salzgehalt und Dichte an der Oberfläche des Atlantischen Ozeans. Wissenschaftliche Ergebnisse der Deutschen Atlantischen Expedition auf dem Forschungs- und Vermessungsschiff "Meteor" 1925–1927, **5**, Atlas.

DEFANT, ALBERT
1936. Die Troposphäre des Atlantischen Ozeans. Idem, **6**, I. Teil, Schichtung und Zirkulation des Atlantischeng Ozeans, pp. 289–411.
1937. Die Ozeanographischen Arbeiten auf der ersten Teilfahrt der Deutschen Nordatlantischen Expedition des "Meteor" Februar bis Mai 1937. *Annalen der Hydrographie und Maritimen Meteorologie*, **65**, Beiheft zum Septemberheft, Bericht über die erste Teilfahrt der Deutschen Nordatlantischen Expedition des Forschungs- und Vermessungsschiff "Meteor" Februar bis Mai 1937, pp. 6–14.

DIETRICH, GÜNTER
1937. I. Die Lage des Meeresoberfläche im Druckfeld von Ozean und Atmosphäre mit besonderer Berücksichtigung des westlichen Nordatlantischen Ozeans und des Golfs von Mexico. II. Über Bewegung und Herkunft des Golfstromwassers. *Veröffentlichungen des Instituts für Meereskunde an der Universität Berlin*, N.F., A, Heft 33.
1937. "Die dynamische Bezugsfläche," ein Gegenwartsproblem der dynamischen Ozeanographie. *Annalen der Hydrographie und Maritimen Meteorologie*, **65**:506–519.

EKMAN, V. W.
1905. On the use of insulated water bottles and reversing thermometers. *Publications de Circonstance*, No. 23.

GRIMMINGER, GEORGE
1938. The intensity of lateral mixing in the atmosphere as determined from isentropic charts. *Transactions of the American Geophysical Union*, Nineteenth Annual Meeting (in press).

ISELIN, C. O'D.
1936. A study of the circulation of the western North Atlantic. *Papers in Physical Oceanography and Meteorology*, **4**, No. 4.

JACOBSEN, J. P.
1929. Contribution to the Hydrography of the North Atlantic. The "Dana" Expedition 1921–22. The Danish "Dana"-Expeditions 1920–22 in the North Atlantic and the Gulf of Panama, No. 3.

KRÜMMEL, OTTO
1907. Die räumlichen, chemischen und physikalischen Verhältnisse des Meeres. Handbuch der Ozeanographie, Verlag von J. Engelhorn, **1**.

MONTGOMERY, R. B.
1936. Transport of surface water due to the wind system over the North Atlantic. *Papers in Physical Oceanography and Meteorology*, **4**, No. 3, On the momentum transfer at the sea surface, pp. 23–30.
1937. A suggested method for representing gradient flow in isentropic surfaces. *Bulletin of the American Meteorological Society*, **18**:210–212.

NAMIAS, JEROME
1938. Thunderstorm forecasting with the aid of isentropic charts. Idem, **19**:1–14.

PARR, A. E.
1936. On the probable relationship between vertical stability and lateral mixing processes. *Journal du Conseil*, **11**:308–313.
1937. A contribution to the hydrography of the Caribbean and Cayman Seas. *Bulletin of the Bingham Oceanographic Collection*, **5**, Art. 4.
1938a. Isopycnic analysis of current flow by means of identifying properties. *Journal of Marine Research*, **1**:133–154.
1938b. Further observations on the hydrography of the eastern Caribbean and adjacent Atlantic waters. *Bulletin of the Bingham Oceanographic Collection*, **6**, Art. 4.

REDFIELD, A. C.
1936. An ecological aspect of the Gulf Stream. *Nature*, **138**:1013.

ROSSBY, C.-G.
1936. Dynamics of steady ocean currents in the light of experimental fluid mechanics. *Papers in Physical Oceanography and Meteorology*, **5**, No. 1.

ROSSBY, C.-G., and MONTGOMERY, R. B.
1935. The layer of frictional influence in wind and ocean currents. Idem, **3**, No. 3.

ROSSBY, C.-G., and collaborators
1937a. Isentropic analysis. *Bulletin of the American Meteorological Society*, **18**:201–209.
1937b. Aerological evidence of large-scale mixing in the atmosphere. *Transactions of the American Geophysical Union*, Eighteenth Annual Meeting, pp. 130–136.

SEIWELL, H. R.
1937a. Short period vertical oscillations in the western basin of the North Atlantic. *Papers in Physical Oceanography and Meteorology*, **5**, No. 2.
1937b. The minimum oxygen concentration in the western basin of the North Atlantic. Idem, **5**, No. 3.

SHAW, NAPIER
1930. The physical processes of weather. Manual of Meteorology, Cambridge University Press, **3**.

SVERDRUP, H. U.
1934. The circulation of the Pacific, *Proceedings of the Fifth Pacific Science Congress*, pp. 2141–2145.

Wüst, Georg
1935. Die Stratosphäre des Atlantischen Ozeans. Wissenschaftliche Ergebnisse der Deutschen Atlantischen Expedition auf dem Forschungs- und Vermessungsschiff "Meteor" 1925–1927, **6**, I. Teil, Schichtung und Zirkulation des Atlantischen Ozeans, pp. 109–288.
Wüst, Georg, und Defant, Albert
1936. Atlas zur Schichtung und Zirkulation des Atlantischen Ozeans. Schnitte und Karten von Temperature, Salzgehalt und Dichte. Idem, **6**, Atlas.

Sources of Hydrographic Data

Atlantis. Reduced data cards of the Woods Hole Oceanographic Institution. Except for stations 2726–2750, these data have been published in *Bulletin Hydrographique*.
Bache. H. B. Bigelow, 1915: Explorations of the United States Coast and Geodetic Survey Steamer "Bache" in the western Atlantic, January–March, 1914, under the direction of the United States Bureau of Fisheries. *Report of the U. S. Commissioner of Fisheries for 1915*, Appendix V.
Carnegie. Reduced data sheets of the Carnegie Institution of Washington, Department of Terrestrial Magnetism.
Challenger. *Bulletin Hydrographique*, 1933, 1934, 1935.
Dana. Johannes Schmidt, 1929: Introduction to the oceanographical reports including list of the stations and hydrographical observations. The Danish "Dana"-Expeditions 1920–22 in the North Atlantic and the Gulf of Panama, No. 1.
Deutschland. Wilhelm Brennecke, 1921: Die oceanographischen Arbeiten der Antarktischen Expedition 1911–1912. *Aus dem Archiv der Deutschen Seewarte*, **39**, Nr. 1.
Discovery. Discovery investigations station list 1925–1927. Discovery Reports, **1**:3–140, 1929.
Discovery II. Discovery investigations station list 1929–1931. Idem, **4**:3–230, 1932.
Meteor, temperature and salinity. Georg Wüst, 1932: Das Ozeanische Beobachtungsmaterial (Serienmessungen). Wissenschaftliche Ergebnisse der Deutschen Atlantischen Expedition auf dem Forschungs- und Vermessungsschiff "Meteor" 1925–1927, **4**, II. Teil.
Meteor, oxygen. Hermann Wattenberg, 1933: Das chemische Beobachtungsmaterial und seine Gewinnung. Idem, **8**.
Michael Sars. Bjørn Helland-Hansen, 1931: Physical oceanography and meteorology. Report on the Scientific Results of the "Michael Sars" North Atlantic Deep-Sea Expedition 1910, **1**.
Möwe. Gerhard Schott und Bruno Schulz, 1914: Die Forschungsreise S.M.S. "Möwe" im Jahre 1911. *Aus dem Archiv der Deutschen Seewarte* **37**:1–80.

CHARTS

Chart 1 shows the locations of all the stations utilized. Charts 2–18 are so arranged that the three on each page give depth, salinity and oxygen distribution for a single σ_t-surface, which is approximately a surface of constant potential density.

The smallest (and horizontal) numbers on Charts 2–19 are the individual station values. Values for a few stations where they are most crowded have been omitted or averaged. The dotted lines on Charts 8–19 represent the mean intersections of the σ_t-surfaces with the sea surface (from Fig. 5). Note that the coastline drawn is the sea surface coastline, not the boundary of the respective σ_t-surface.

On the charts at the top of the following pages, showing depth in meters, Chart 2 with lines for every 100 meters and Charts 5, 8, 11, 14, 17 with lines for every 50 meters, the symbol "D" designates a dome or ridge, "T" a trough or depression. The broken lines on Charts 5, 8, 11, 14, 17 are the mean March and September positions of the intersections of the respective σ_t-surfaces with the sea surface. Station values on charts 2 and 5 are in tens of meters.

On the charts in the middle of the following pages, showing salinity with lines for every 0.1 $^0/_{00}$, the symbol "S" designates a region of high salinity, especially the source or upstream end of a salt tongue; conversely "F" designates relatively fresh water. On charts 9, 12, 15, 18 the small slanting numbers along the dotted line give the mean salinity at the sea surface (from Fig. 5).

On the charts at the bottom of the following pages, showing O_2-content with lines for every 0.5 cc.l.$^{-1}$, the symbol "R" designates water rich in oxygen, especially the source or upstream end of a rich tongue; conversely "P" designates water poor in oxygen.

The arrows are identical on the three charts for each σ_t-surface. "These represent primarily the axes of tongues of salt or fresh water or of water rich or poor in oxygen. Some of them represent current axes also. Arrows with broken shafts represent trajectories of temporary nature or those whose existence is more doubtful." (cf. p. 26.) 2nd ¶ up

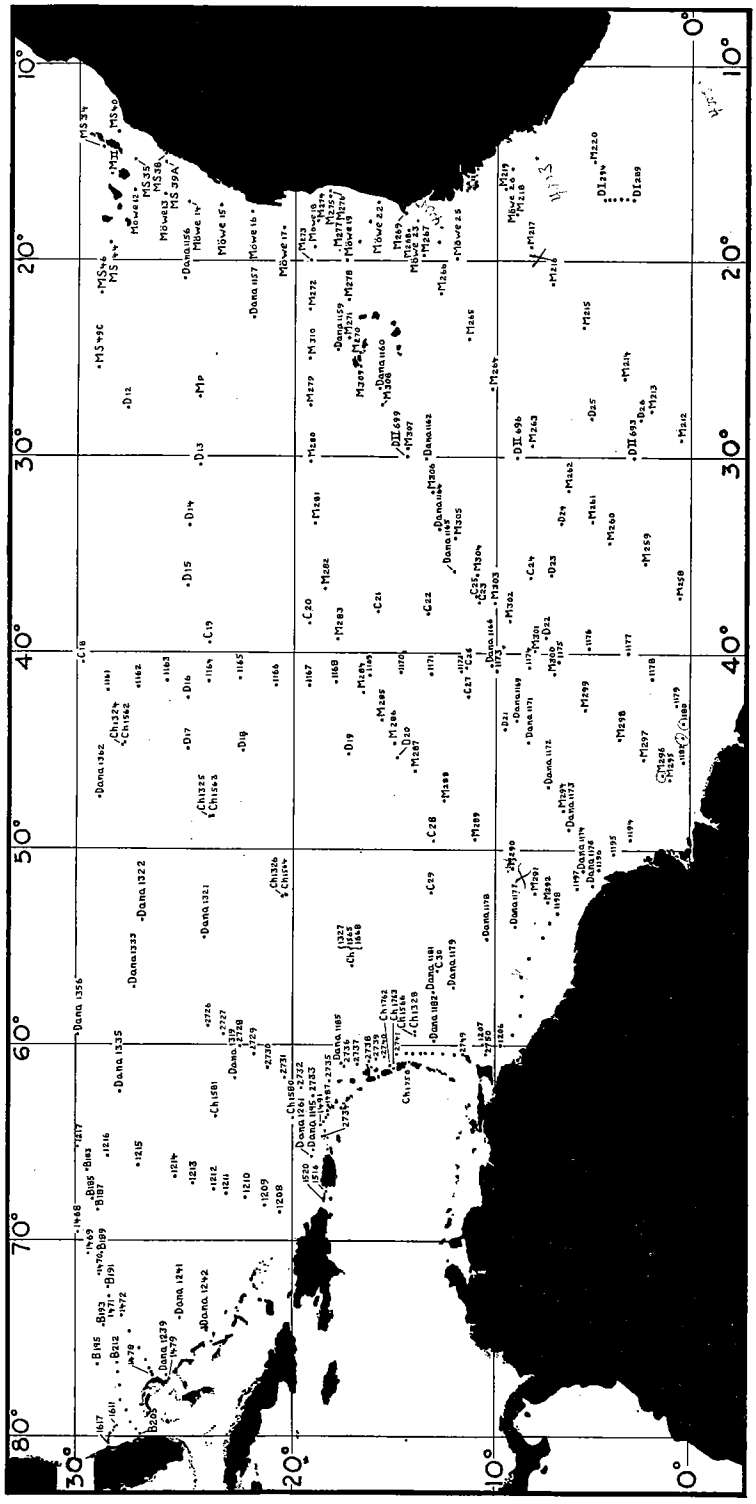

CHART I.—Locations of stations. Unlettered: *Atlantis*, B: *Bache*, C: *Carnegie*, Ch: *Challenger* (1933–1935), D: *Deutschland* (Reihe), DI: *Discovery*, DII: *Discovery II*, M: *Meteor*, MS: *Michael Sars*.

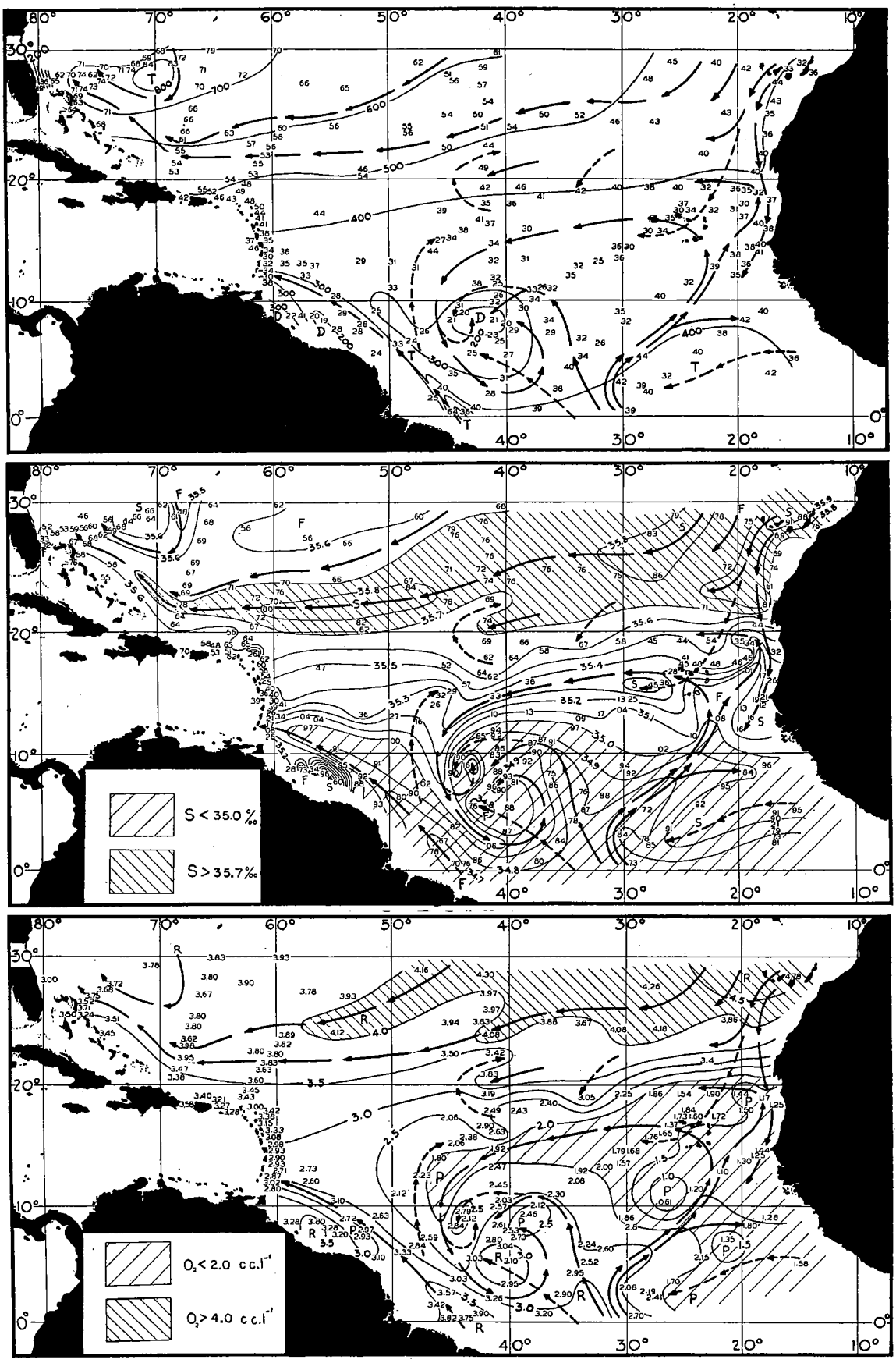

CHARTS 2–4.—Depth, salinity and oxygen at $\sigma_t = 27$. Whole numbers (34 or 35) omitted from station salinities.

$\delta_t = 106.7$

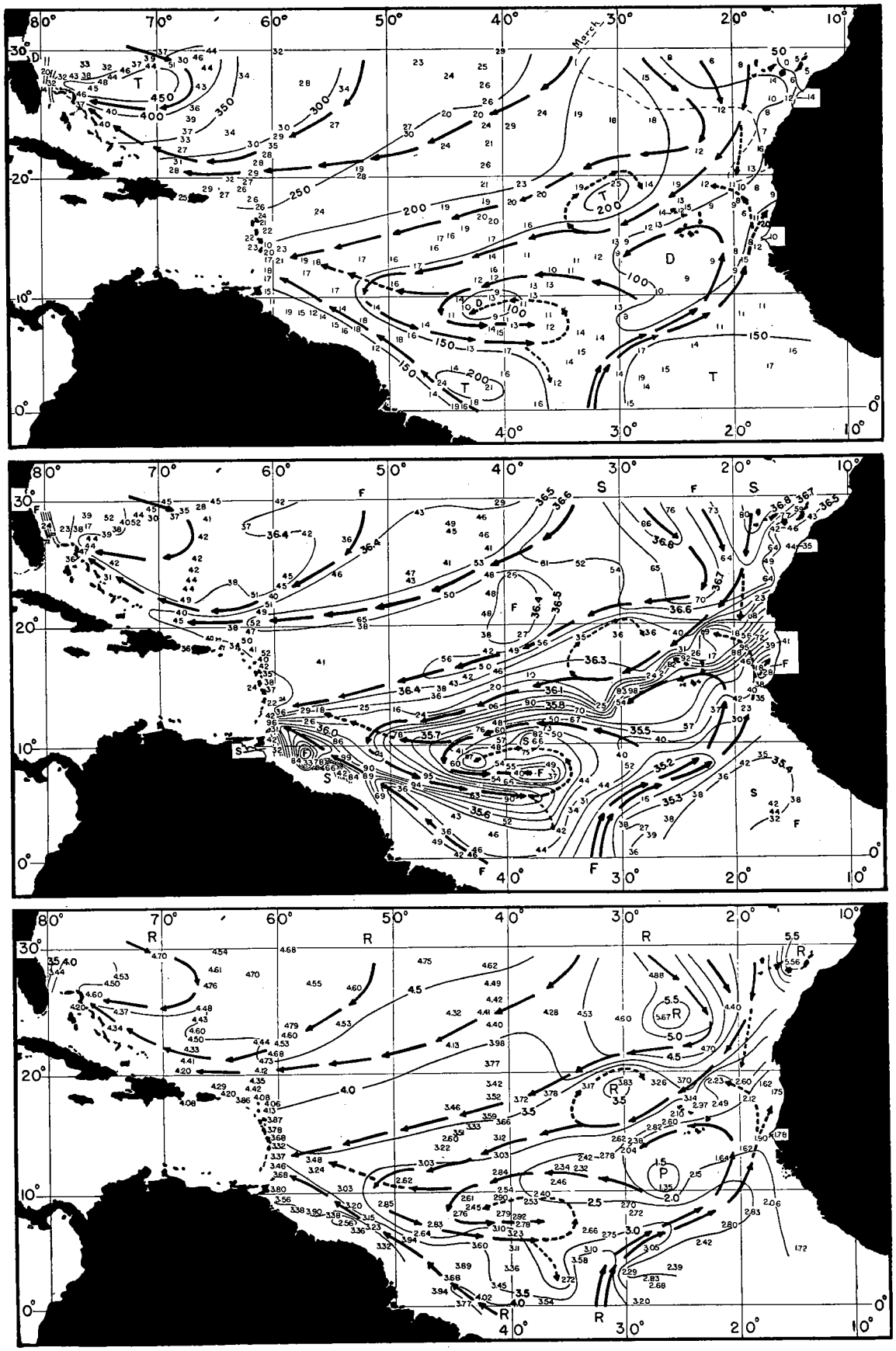

CHARTS 5–7.—Depth, salinity and oxygen at $\sigma_t = 26.5$. Whole numbers (35 or 36) omitted from station salinities.

δ_t - 15·1.1

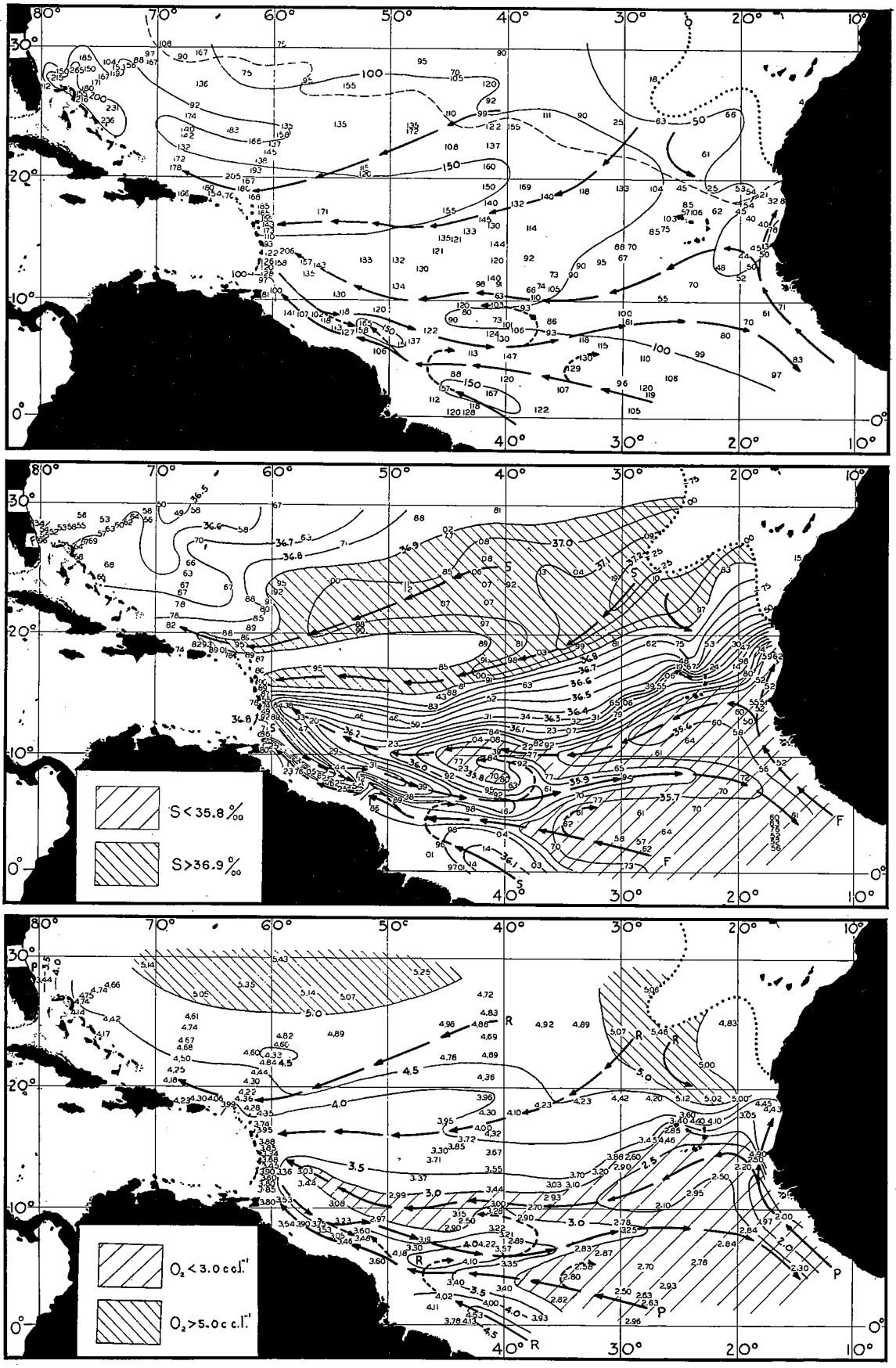

CHARTS 8–10.—Depth, salinity and oxygen at $\sigma_t = 26$. Whole numbers (35 or 36 or 37) omitted from station salinities.

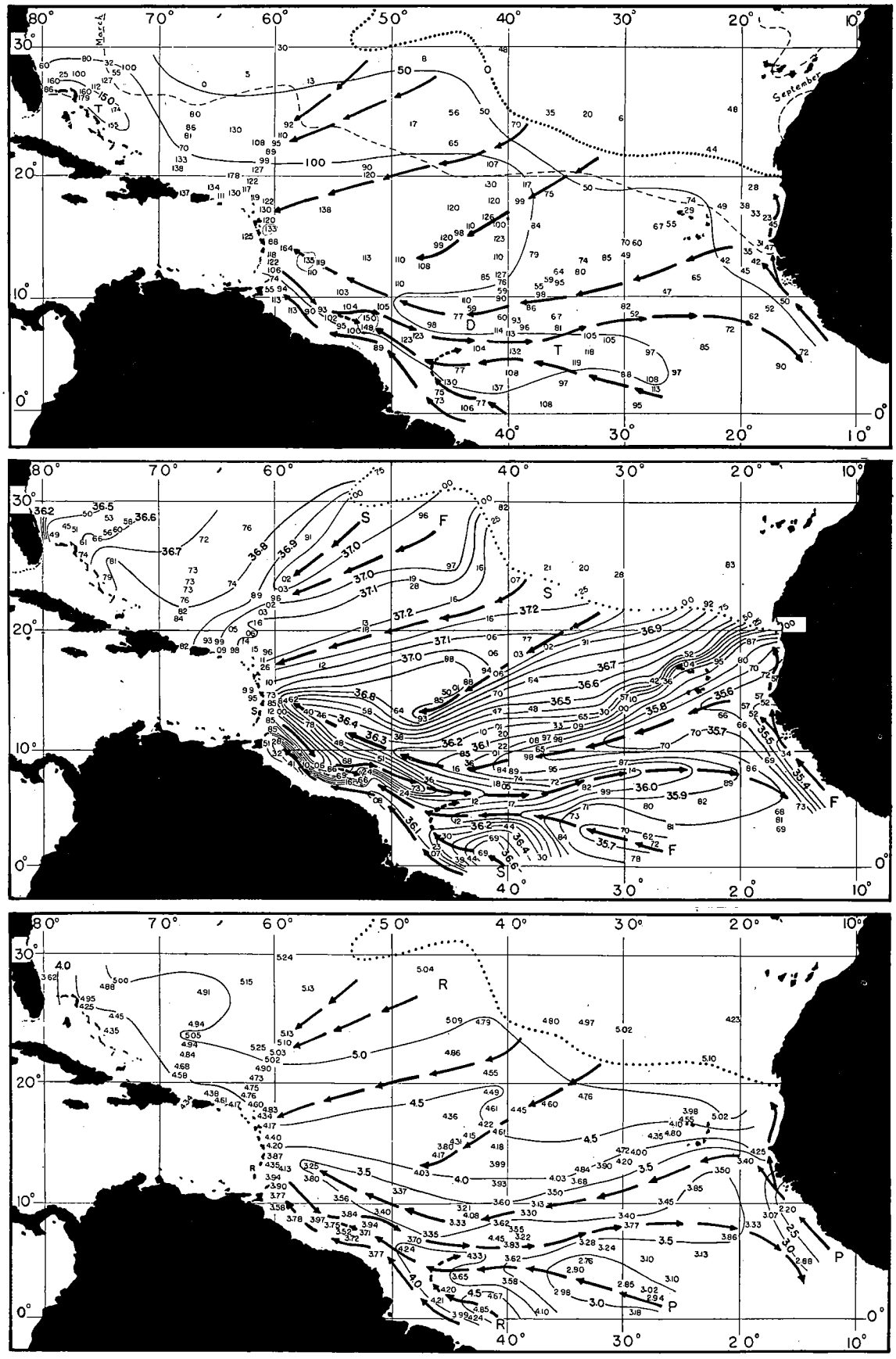

CHARTS 11–13.—Depth, salinity and oxygen at $\sigma_t = 25.5$. Whole numbers (35 or 36 or 37) omitted from station salinities.

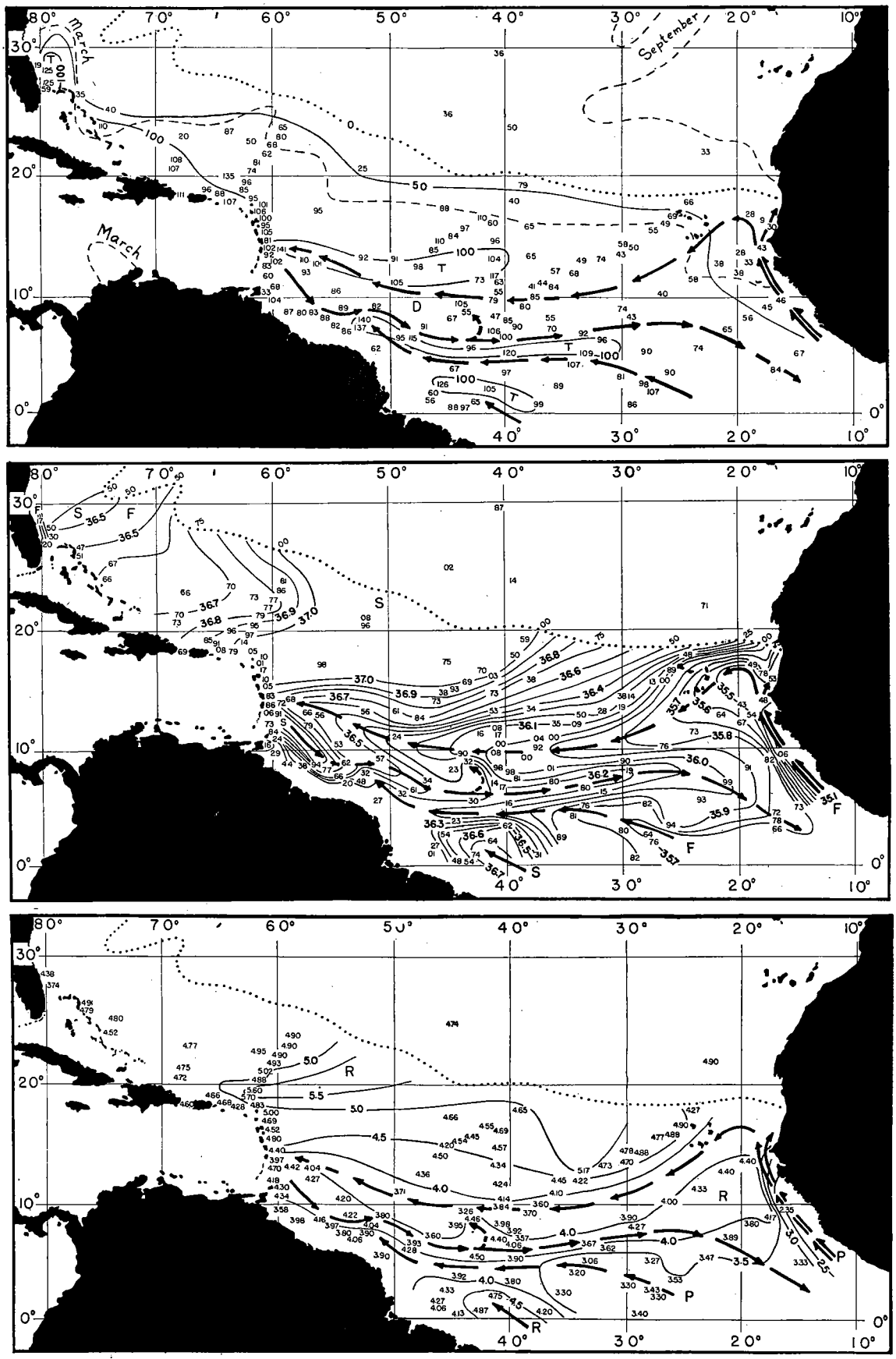

CHARTS 14–16.—Depth, salinity and oxygen at $\sigma_t = 25$. Whole numbers (35 or 36 or 37) omitted from station salinities.

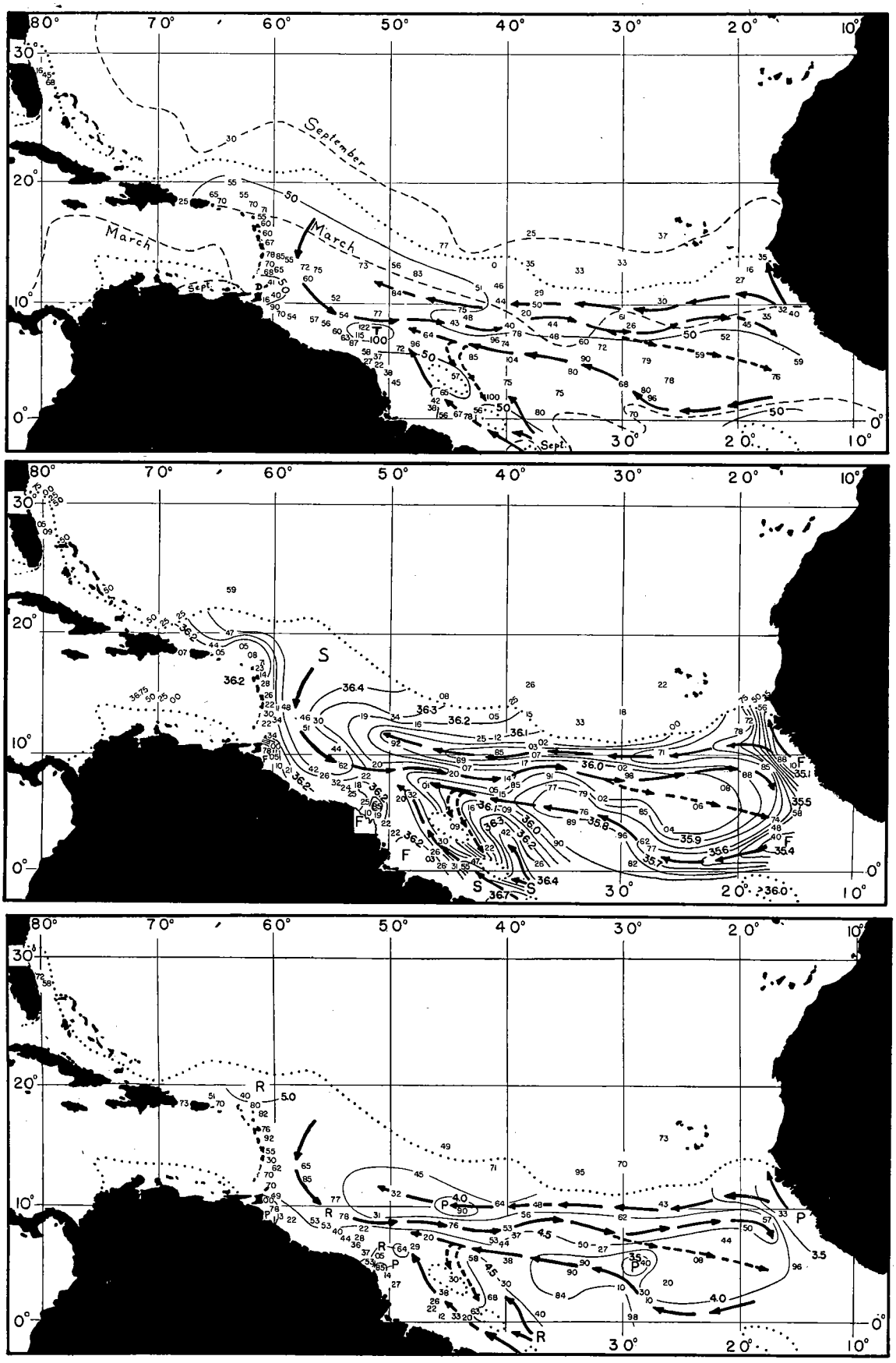

CHARTS 17–19.—Depth, salinity and oxygen at $\sigma_t = 24.$ 34 or 35 or 36 omitted from salinities, 3 or 4 or 5 from oxygens.